

**A Method for the Efficient Construction of Acoustic Pressure
Cross-Spectral Matrices**

S.H. Yoon and P.A. Nelson

ISVR Technical Report No 281

October 1998



SCIENTIFIC PUBLICATIONS BY THE ISVR

Technical Reports are published to promote timely dissemination of research results by ISVR personnel. This medium permits more detailed presentation than is usually acceptable for scientific journals. Responsibility for both the content and any opinions expressed rests entirely with the author(s).

Technical Memoranda are produced to enable the early or preliminary release of information by ISVR personnel where such release is deemed to be appropriate. Information contained in these memoranda may be incomplete, or form part of a continuing programme; this should be borne in mind when using or quoting from these documents.

Contract Reports are produced to record the results of scientific work carried out for sponsors, under contract. The ISVR treats these reports as confidential to sponsors and does not make them available for general circulation. Individual sponsors may, however, authorize subsequent release of the material.

COPYRIGHT NOTICE

(c) ISVR University of Southampton All rights reserved.

ISVR authorises you to view and download the Materials at this Web site ("Site") only for your personal, non-commercial use. This authorization is not a transfer of title in the Materials and copies of the Materials and is subject to the following restrictions: 1) you must retain, on all copies of the Materials downloaded, all copyright and other proprietary notices contained in the Materials; 2) you may not modify the Materials in any way or reproduce or publicly display, perform, or distribute or otherwise use them for any public or commercial purpose; and 3) you must not transfer the Materials to any other person unless you give them notice of, and they agree to accept, the obligations arising under these terms and conditions of use. You agree to abide by all additional restrictions displayed on the Site as it may be updated from time to time. This Site, including all Materials, is protected by worldwide copyright laws and treaty provisions. You agree to comply with all copyright laws worldwide in your use of this Site and to prevent any unauthorised copying of the Materials.

UNIVERSITY OF SOUTHAMPTON
INSTITUTE OF SOUND AND VIBRATION RESEARCH
FLUID DYNAMICS AND ACOUSTICS GROUP

**A Method for the Efficient Construction of Acoustic
Pressure Cross-Spectral Matrices**

by

S H Yoon and P A Nelson

ISVR Technical Report No. 281

October 1998

Authorized for issue by
Professor P A Nelson
Group Chairman

© Institute of Sound & Vibration Research

CONTENTS

1. Introduction
2. Theoretical Development
 - 2.1 Use of Reference Microphones
 - 2.2 The Moving Position Cross-Spectral Matrix S_{MM}
3. A Simple Example
4. Estimation of the Rank
 - 4.1 Introduction
 - 4.2 Principal Component Analysis
 - 4.3 Virtual Coherence
5. Relation between the Rank of Acoustic Pressure Cross-Spectral Matrix and the Number of Uncorrelated Acoustic Sources
6. Rank Equality and the Choice of the Number of Reference Microphones
7. Simulation Results I: No Measurement Noise
 - 7.1 Uncorrelated Acoustic Source Strengths
 - 7.2 Correlated Acoustic Source Strengths
8. Simulation Results II: With Output Noise
 - 8.1 Uncorrelated Acoustic Source Strengths
 - 8.2 Correlated Acoustic Source Strengths
9. Experimental Verification
10. Conclusions

Acknowledgement

References

Appendix: Proof of Equation (31)

FIGURES

Figure 1. The partition of the entire number of measurement positions (or microphones) into the reference and moving positions (or microphones).

Figure 2. A simulation model for computing the ranks of S_{RR} , S_{RM} , S_I , and S_{pp} .

Figure 3. Effect of the number of reference microphones ((a) 3, (b) 4, (c) 5) on variations of rank of S_{pp} (solid), rank of S_I (circle) and the normalised difference R_1 . There are 4 uncorrelated acoustic sources.

Figure 4. Principal auto-spectra (or singular values) of S_{pp} for the model (Figure 2) comprising 4 uncorrelated sources under the assumption of no output noise.

Figure 5. Virtual coherences of the 1st (black thick), the 2nd (grey thick), the 3rd (black thin), and the 4th (grey thin) virtual acoustic pressure with respect to the physical acoustic pressure sensed at the microphone 1 for the model in Figure 2 comprising 4 uncorrelated sources and the assumption of no output noise.

Figure 6. A comparison of the directly calculated (solid) and estimated (dotted) S_{MM} : (a) auto-spectra at the 1st moving position, (b) auto-spectra at the 4th moving position, (c) (d) magnitude and phase of cross-spectra between the 1st and 4th moving positions, (e) normalised difference R_1 , (f) normalised difference matrix R_2 at $kr_{ss}=1.65$ ($=600\text{Hz}$, $r_{ss}=0.15\text{m}$). These results are for the model of Figure 2 comprising 4 uncorrelated sources and the assumption of no output noise.

Figure 7. Geometry of a simply supported plate mounted in an infinite baffle used for the computer simulation.

Figure 8. Principal auto-spectra (or singular values) of S_{pp} for the simply supported plate model (Figure 7) under the assumption of no output noise.

Figure 9. Virtual coherence of the virtual acoustic pressure with respect to the physical acoustic pressure sensed at the microphone 1 for the simply supported plate model (Figure 7) under the assumption of no output noise.

Figure 10. A comparison of the directly calculated (solid) and estimated (dotted) S_{MM} : (a) auto-spectra at the 1st moving position, (b) auto-spectra at the 4th moving position, (c) (d) magnitude and phase of cross-spectra between the 1st and 4th moving positions, (e) normalised difference R_1 , (f) normalised difference matrix R_2 at $kr_{ss}=1.37$ ($=786\text{Hz}$, $r_{ss}=0.095\text{m}$) which is the (2,3) resonant frequency. These results are for the simply supported

plate model of Figure 7 under the assumption of no output noise.

Figure 11. Principal auto-spectra (or singular values) of $\mathbf{S}_{\hat{p}\hat{p}}$ for the model of Figure 2.

Figure 12. A comparison of the directly calculated (solid) and estimated (dotted) $\mathbf{S}_{\hat{M}\hat{M}}$: (a) auto-spectra at the 1st moving position, (b) auto-spectra at the 4th moving position, (c) (d) magnitude and phase of cross-spectra between the 1st and 4th moving positions, (e) normalised difference R_1 , (f) normalised difference matrix \mathbf{R}_2 at $kr_{ss}=1.65$ ($=600\text{Hz}$, $r_{ss}=0.15\text{m}$) for the model of Figure 2 with output noise. Four reference microphones are used.

Figure 13. A comparison of the directly calculated (solid) and estimated (dotted) $\mathbf{S}_{\hat{M}\hat{M}}$: (a) auto-spectra at the 1st moving position, (b) auto-spectra at the 4th moving position, (c) (d) magnitude and phase of cross-spectra between the 1st and 4th moving positions, (e) normalised difference R_1 , (f) normalised difference matrix \mathbf{R}_2 at $kr_{ss}=1.65$ ($=600\text{Hz}$, $r_{ss}=0.15\text{m}$). These results are for the model of Figure 2 with output noise when 5 reference microphones are used.

Figure 14. Principal auto-spectra (or singular values) of $\mathbf{S}_{\hat{p}\hat{p}}$ for the model of Figure 7.

Figure 15. A comparison of the directly calculated (solid) and estimated (dotted) $\mathbf{S}_{\hat{M}\hat{M}}$: (a) auto-spectra at the 1st moving position, (b) auto-spectra at the 4th moving position, (c) (d) magnitude and phase of cross-spectra between the 1st and 4th moving positions, (e) normalised difference R_1 , (f) normalised difference matrix \mathbf{R}_2 at $kr_{ss}=1.37$ ($=786\text{Hz}$, $r_{ss}=0.095\text{m}$) which is the (2,3) resonant frequency for the simply supported plate model of Figure 7 with output noise. One reference microphone is used.

Figure 16. A comparison of the directly calculated (solid) and estimated (dotted) $\mathbf{S}_{\hat{M}\hat{M}}$: (a) auto-spectra at the 1st moving position, (b) auto-spectra at the 4th moving position, (c) (d) magnitude and phase of cross-spectra between the 1st and 4th moving positions, (e) normalised difference R_1 , (f) normalised difference matrix \mathbf{R}_2 at $kr_{ss}=1.37$ ($=786\text{Hz}$, $r_{ss}=0.095\text{m}$) which is the (2,3) resonant frequency. These results are for the simply supported plate model of Figure 7 with output noise. Two reference microphones are used.

Figure 17. Experimental arrangement for the reconstruction of strengths of two volume velocity sources.

Figure 18. Experimental arrangement for the reconstruction of volume velocities of a randomly vibrating plate mounted in a finite baffle.

Figure 19. Six principal auto-spectra (or singular values) of $\mathbf{S}_{\hat{p}\hat{p}}$ for the model (Figure 17) consisting of the two volume velocity sources driven by one random noise generator and six microphones.

Figure 20. Virtual coherences of the 1st to 6th virtual acoustic pressure with respect to the physical acoustic pressure sensed at the microphone 1 in Figure 20(b) consisting of the two volume velocity sources driven by one random noise generator and six microphones.

Figure 21. A comparison of the directly measured (solid) and estimated (dotted) $S_{\hat{M}\hat{M}}$: (a) auto-spectra at the 1st moving position, (b) auto-spectra at the 2nd moving position, (c) (d) magnitude and phase of cross-spectra between the 1st and 2nd moving positions, (e) normalised difference R_1 , (f) normalised difference matrix \mathbf{R}_2 at $ka=0.1$ ($=400\text{Hz}$, $a=0.014\text{m}$) for the model of Figure 17 consisting of the two volume velocity sources driven by one random noise generator and six microphones. One reference microphone is used.

Figure 22. Principal auto-spectra (or singular values) of $S_{\hat{p}\hat{p}}$ for the model (Fig. 9.13) consisting of the simply supported plate excited by one electromagnetic driver and four microphones.

Figure 23. Virtual coherences of the 1st (black thick), the 2nd (grey thick), the 3rd (black thin), and the 4th virtual acoustic pressure (grey thin circle) with respect to the physical acoustic pressure sensed at the microphone 1 in Figure 18 consisting of the simply supported plate excited by one electromagnetic driver and four microphones.

Figure 24. A comparison of the directly measured (solid) and estimated (dotted) $S_{\hat{M}\hat{M}}$: (a) auto-spectra at the 1st moving position, (b) auto-spectra at the 2nd moving position, (c) (d) magnitude and phase of cross-spectra between the 1st and 2nd moving positions, (e) normalised difference R_1 , (f) normalised difference matrix \mathbf{R}_2 at $ka=0.1$ ($=458\text{Hz}$, $a=0.014\text{m}$) for the model of Figure 18 consisting of the simply supported plate excited by one electromagnetic driver. One reference microphone is used.

Figure 25. A comparison of the directly measured (solid) and estimated (dotted) $S_{\hat{M}\hat{M}}$: (a) auto-spectra at the 1st moving position, (b) auto-spectra at the 2nd moving position, (c) (d) magnitude and phase of cross-spectra between the 1st and 2nd moving positions, (e) normalised difference R_1 , (f) normalised difference matrix \mathbf{R}_2 at $ka=0.1$ ($=458\text{Hz}$, $a=0.014\text{m}$) for the model of Figure 18 consisting of the simply supported plate excited by one electromagnetic driver. Two reference microphones are used.

ABSTRACT

A method is presented for constructing, with the minimum number of physical measurements, the full cross-spectral matrix of acoustic pressures associated with a number of measurement positions. It is necessary to evaluate the elements of the matrix in question when using inverse methods for the reconstruction of acoustic source strength spectra. The method presented uses the concept of “reference microphones”. The relation between the rank of the cross-spectral matrix of acoustic pressures and the number of uncorrelated acoustic sources is discussed and used to determine the required number of reference microphones. A method is proposed for selecting this number in the inverse problem in which information regarding acoustic sources is unknown. The results of computer simulations are presented which explore the main features of the technique under various conditions. Experimental results are also presented which validate the technique.

1. INTRODUCTION

In order to reconstruct the cross-spectral matrix of acoustic source strengths by inverse techniques, it is necessary to first measure the cross-spectral matrix of acoustic pressures in the radiated sound field [1, 2]. This matrix can be constructed by measuring directly all auto-spectra at the field points considered and the cross-spectra between all pairs of field points. However, this often leads to a tedious and expensive task, especially when the number of field points is large. For example, when we wish to measure acoustic pressure auto- and cross-spectra at 100 field points by using dual channel acquisition equipment, then the dimension of the matrix of acoustic pressure auto- and cross-spectra becomes 100-by-100 and thus we need 5050 measurements ($=100 \times 101/2$, since this matrix is an Hermitian matrix). In this case, it is natural to attempt to develop an alternative technique which constructs the full auto- and cross-spectral matrix of acoustic pressures with a minimum number of measurements. This report proposes such a technique using a small number of reference microphones.

Hald [3], in developing the application of Nearfield Acoustic Holography (NAH), adopted the concept of the reference microphone, with a view to obtaining the full cross-spectral matrix with a minimum number of measurements of acoustic pressure cross-spectra on the “hologram plane”. We also employ the concept of the reference microphone to construct the full cross-spectral matrix of acoustic pressures with a minimum number of measurements on the “measurement plane”. Although our work adopts the concept of the reference microphone as used by Hald, there are important differences. First of all, here we divide “conceptually” the entire number of measurement microphones (or number of measurement positions) into reference microphones (or reference positions) and moving microphones (or moving positions) on the measurement plane. However, Hald “actually” used reference microphones which are located between acoustic sources and scanning microphones on the hologram plane. In our work, the full cross-spectral matrix of acoustic pressures on the measurement plane comprises constructions from both the reference and moving positions (or microphones). On the contrary, in Hald’s work, the full cross-spectral matrix of acoustic pressures consists of only the auto- and cross-spectral matrix of acoustic pressures measured on the hologram plane, not including that sensed by

reference microphones. Furthermore, our mathematical development differs from that presented by Hald.

In this report, the theoretical development of this technique is presented by employing the concept of the rank of a matrix. The heart of this technique is the proof of the rank equality between the matrix of acoustic pressure cross-spectra measured at the entire number of field points and a certain sub-matrix of acoustic pressure cross-spectra. To verify the rank equality, it is first necessary to understand the relation between the rank of the acoustic pressure cross-spectral matrix and the number of uncorrelated acoustic sources, and this is therefore described. Also, some methods for the estimation of the ranks of these matrices are discussed. They are eigenvalue decomposition, singular value decomposition, principal component analysis and virtual coherence. It is crucial, in securing the rank equality referred to above, to select properly the number of reference microphones. Accordingly, a method is proposed for selecting this number in an inverse problem in which information regarding acoustic sources is unknown. In order to clarify the main features of the theory developed, the results of computer simulations are presented for the problems in which acoustic sources are either mutually uncorrelated or correlated and in which the effect of output noise is also included. Finally this technique is validated from experiments which use the acoustic pressures radiated from the two volume velocity sources and a simply supported plate mounted in a finite baffle.

2. THEORETICAL DEVELOPMENT

2.1 USE OF REFERENCE MICROPHONES

When we assume that there is no measurement noise, the m -dimensional complex vector \mathbf{p} of desired acoustic pressures is related to the n -dimensional complex vector \mathbf{q} of acoustic source strength by using the m -by- n complex matrix \mathbf{H} of transfer functions and thus

$$\mathbf{p} = \begin{bmatrix} p_1(\omega) \\ p_2(\omega) \\ \vdots \\ \vdots \\ p_m(\omega) \end{bmatrix} = \begin{bmatrix} H_{11}(\omega) & H_{12}(\omega) & \cdots & H_{1n}(\omega) \\ H_{21}(\omega) & H_{22}(\omega) & \cdots & H_{2n}(\omega) \\ \vdots & \vdots & & \vdots \\ \vdots & \vdots & & \vdots \\ H_{m1}(\omega) & H_{m2}(\omega) & \cdots & H_{mn}(\omega) \end{bmatrix} \begin{bmatrix} q_1(\omega) \\ q_2(\omega) \\ \vdots \\ \vdots \\ q_n(\omega) \end{bmatrix} = \mathbf{H}\mathbf{q}. \quad (1)$$

Now, as can be seen from Figure 1, we conceptually partition the complex vector \mathbf{p} consisting of acoustic pressures sensed at the entire number of measurement positions into a complex vector \mathbf{p}_R which contains acoustic pressures measured at u reference positions and a complex vector \mathbf{p}_M which consists of acoustic pressures measured at v moving positions such that

$$\mathbf{p}_R = \begin{bmatrix} p_1(\omega) \\ p_2(\omega) \\ \vdots \\ \vdots \\ p_u(\omega) \end{bmatrix}, \quad \mathbf{p}_M = \begin{bmatrix} p_1(\omega) \\ p_2(\omega) \\ \vdots \\ \vdots \\ p_v(\omega) \end{bmatrix}. \quad (2, 3)$$

It is now assumed that the transfer function matrices \mathbf{H}_R and \mathbf{H}_M relate the acoustic source strengths \mathbf{q} to the acoustic pressures \mathbf{p}_R and \mathbf{p}_M at the reference and moving positions, respectively. Thus

$$\mathbf{p}_R = \begin{bmatrix} p_1(\omega) \\ p_2(\omega) \\ \vdots \\ \vdots \\ p_u(\omega) \end{bmatrix} = \begin{bmatrix} H_{11}(\omega) & H_{12}(\omega) & \cdots & H_{1n}(\omega) \\ H_{21}(\omega) & H_{22}(\omega) & \cdots & H_{2n}(\omega) \\ \vdots & \vdots & & \vdots \\ \vdots & \vdots & & \vdots \\ H_{u1}(\omega) & H_{u2}(\omega) & \cdots & H_{un}(\omega) \end{bmatrix} \begin{bmatrix} q_1(\omega) \\ q_2(\omega) \\ \vdots \\ \vdots \\ q_n(\omega) \end{bmatrix} = \mathbf{H}_R \mathbf{q}, \quad (4)$$

and

$$\mathbf{p}_M = \begin{bmatrix} p_1(\omega) \\ p_2(\omega) \\ \vdots \\ \vdots \\ p_v(\omega) \end{bmatrix} = \begin{bmatrix} H_{11}(\omega) & H_{12}(\omega) & \cdots & H_{1n}(\omega) \\ H_{21}(\omega) & H_{22}(\omega) & \cdots & H_{2n}(\omega) \\ \vdots & \vdots & & \vdots \\ \vdots & \vdots & & \vdots \\ H_{v1}(\omega) & H_{v2}(\omega) & \cdots & H_{vn}(\omega) \end{bmatrix} \begin{bmatrix} q_1(\omega) \\ q_2(\omega) \\ \vdots \\ \vdots \\ q_n(\omega) \end{bmatrix} = \mathbf{H}_M \mathbf{q}. \quad (5)$$

Accordingly, from equations (1), (4) and (5), we can express the relationship of \mathbf{p}_R , \mathbf{p}_M and \mathbf{p} as

$$\mathbf{p} = \begin{bmatrix} \mathbf{p}_R \\ \mathbf{p}_M \end{bmatrix} = \begin{bmatrix} p_1(\omega) \\ p_2(\omega) \\ \vdots \\ p_u(\omega) \\ p_{u+1}(\omega) \\ p_{u+2}(\omega) \\ \vdots \\ p_{u+v}(\omega) \end{bmatrix} = \begin{bmatrix} \mathbf{H}_R \\ \mathbf{H}_M \end{bmatrix} \mathbf{q} = \mathbf{H} \mathbf{q} , \quad (6)$$

where the entire number m of measurement positions is equal to sum of the number u of reference positions and the number v of moving positions, namely, $m=u+v$. With the vector \mathbf{p} partitioned as in equation (6), we can obtain the acoustic pressure auto- and cross-spectral matrix \mathbf{S}_{pp} expressed as

$$\mathbf{S}_{pp} = [\mathbf{p} \mathbf{p}^H] = \begin{bmatrix} \mathbf{p}_R \mathbf{p}_R^H & \mathbf{p}_R \mathbf{p}_M^H \\ \mathbf{p}_M \mathbf{p}_R^H & \mathbf{p}_M \mathbf{p}_M^H \end{bmatrix} . \quad (7)$$

Now define the u -by- u matrix \mathbf{S}_{RR} (reference position cross-spectral matrix), the u -by- v matrix \mathbf{S}_{RM} (reference-moving position cross-spectral matrix) and the v -by- v matrix \mathbf{S}_{MM} (moving position cross-spectral matrix) in the form

$$\mathbf{S}_{RR} = [\mathbf{p}_R \mathbf{p}_R^H] , \quad (8)$$

$$\mathbf{S}_{RM} = [\mathbf{p}_R \mathbf{p}_M^H] , \quad (9)$$

and

$$\mathbf{S}_{MM} = [\mathbf{p}_M \mathbf{p}_M^H] . \quad (10)$$

These matrices enable the m -by- m (or $(u+v)$ -by- $(u+v)$) matrix \mathbf{S}_{pp} given by equation (7) to be expressed in the form

$$\mathbf{S}_{pp} = \begin{bmatrix} \mathbf{S}_{RR} & \mathbf{S}_{RM} \\ \mathbf{S}_{RM}^H & \mathbf{S}_{MM} \end{bmatrix} . \quad (11)$$

Note that the analysis resulting in equation (11) is for acoustic pressures that have a deterministic time history. For acoustic pressures that have a time dependence which can be regarded as random with stationary statistical properties, \mathbf{S}_{pp} is given by

$$\mathbf{S}_{pp} = E[\mathbf{p}\mathbf{p}^H] = E \begin{bmatrix} \mathbf{p}_R \mathbf{p}_R^H & \mathbf{p}_R \mathbf{p}_M^H \\ \mathbf{p}_M \mathbf{p}_R^H & \mathbf{p}_M \mathbf{p}_M^H \end{bmatrix}. \quad (12)$$

where the expectation operator $E[\bullet]$ is taken to mean the abbreviation of $\lim_{T \rightarrow \infty} \frac{1}{T} E[\bullet]$.

In this case, \mathbf{S}_{RR} , \mathbf{S}_{RM} and \mathbf{S}_{MM} are expressed as

$$\mathbf{S}_{RR} = E[\mathbf{p}_R \mathbf{p}_R^H], \quad (13)$$

$$\mathbf{S}_{RM} = E[\mathbf{p}_R \mathbf{p}_M^H], \quad (14)$$

and

$$\mathbf{S}_{MM} = E[\mathbf{p}_M \mathbf{p}_M^H]. \quad (15)$$

Using these matrices, we again have the same matrix \mathbf{S}_{pp} as equation (11).

To construct all the components of \mathbf{S}_{pp} given by equation (11), we undertake the following procedure: we first *measure* the reference position auto- and cross-spectral matrix \mathbf{S}_{RR} and the reference-moving position cross-spectral matrix \mathbf{S}_{RM} , then *calculate* the moving position auto- and cross-spectral matrix \mathbf{S}_{MM} from the measured \mathbf{S}_{RR} and \mathbf{S}_{RM} . Hence the measurement of only \mathbf{S}_{RR} and \mathbf{S}_{RM} is required in constructing the full matrix of \mathbf{S}_{pp} . In the next section we describe how to calculate the matrix \mathbf{S}_{MM} .

2.2 THE MOVING POSITION CROSS-SPECTRAL MATRIX \mathbf{S}_{MM}

Let the first u columns of \mathbf{S}_{pp} be represented by m -by- u (or $(u+v)$ -by- u) matrix \mathbf{S}_1 and the remaining columns m -by- v (or $(u+v)$ -by- v) matrix \mathbf{S}_2 , respectively. Thus,

$$\mathbf{S}_1 = \begin{bmatrix} \mathbf{S}_{RR} \\ \mathbf{S}_{RM}^H \end{bmatrix}, \quad (16)$$

$$\mathbf{S}_2 = \begin{bmatrix} \mathbf{S}_{RM} \\ \mathbf{S}_{MM} \end{bmatrix}. \quad (17)$$

Therefore, the matrix \mathbf{S}_{pp} can be expressed as

$$\mathbf{S}_{pp} = [\mathbf{S}_1 \quad \mathbf{S}_2] \quad . \quad (18)$$

To calculate the moving position auto- and cross-spectral matrix \mathbf{S}_{MM} from the measured matrices \mathbf{S}_{RR} and \mathbf{S}_{RM} , we have to *assume* the rank equality of \mathbf{S}_1 and \mathbf{S}_{pp} , i.e.,

$$\text{rank}(\mathbf{S}_{pp}) = \text{rank}(\mathbf{S}_1) \quad . \quad (19)$$

If this is the case, since the matrix \mathbf{S}_2 does not contribute to the rank of the matrix \mathbf{S}_{pp} , the columns of \mathbf{S}_2 in equation (18) can be expressed by linear combinations of the columns of \mathbf{S}_1 . Accordingly (see reference [4]), there exists a u -by- v matrix \mathbf{T} enabling \mathbf{S}_2 to be written as

$$\mathbf{S}_2 = \mathbf{S}_1 \mathbf{T} \quad . \quad (20)$$

Using equations (16) and (17), equation (20) can also be expressed as

$$\mathbf{S}_{RM} = \mathbf{S}_{RR} \mathbf{T} \quad , \quad (21)$$

$$\mathbf{S}_{MM} = \mathbf{S}_{RM}^H \mathbf{T} \quad . \quad (22)$$

Arranging equation (21) with respect to \mathbf{T} and substituting this into equation (22), we can find the moving position auto- and cross-spectral matrix \mathbf{S}_{MM} . Thus

$$\mathbf{S}_{MM} = \mathbf{S}_{RM}^H \mathbf{S}_{RR}^{-1} \mathbf{S}_{RM} \quad . \quad (23)$$

Note that equation (23) is valid only when \mathbf{S}_{RR} is of full rank, otherwise the generalised inverse has to be employed instead of the direct inverse. Thus

$$\mathbf{S}_{MM} = \mathbf{S}_{RM}^H \mathbf{S}_{RR}^+ \mathbf{S}_{RM} \quad . \quad (24)$$

Consequently, in constructing the full matrix \mathbf{S}_{pp} , if we use this procedure rather than direct measurement, then we can take advantage of a great reduction in the number of required measurements. That is to say, while the number of required direct measurements is $(u+v)(u+v+1)/2$ (because the dimension of \mathbf{S}_{pp} is $(u+v)$ -by- $(u+v)$ and this is an Hermitian matrix), the technique proposed here needs only $u(u+1)/2$ (because the dimension of \mathbf{S}_{RR} is u -by- u and this is an Hermitian matrix) plus uv

(because the dimension of \mathbf{S}_{RM} is u -by- v). When $u=5$ and $v=95$, for example, the number of required direct measurements is 5050, but this technique reduces that to 490. Of course, these numbers are computed under the condition in which we use data acquisition equipment with dual channels, and therefore when we use multi-channel equipment, the number of required measurements will be reduced. However, in utilising equations (23) or (24), it should be emphasised that it is a prerequisite to validate the assumed rank equality between \mathbf{S}_1 and \mathbf{S}_{pp} .

3. A SIMPLE EXAMPLE

To help understand the technique using reference microphones, we consider a simple example consisting of one acoustic source and three field points numbered 1, 2 and 3 such that

$$\mathbf{p} = \begin{bmatrix} p_1 \\ p_2 \\ p_3 \end{bmatrix} = \begin{bmatrix} H_1 \\ H_2 \\ H_3 \end{bmatrix} q = \mathbf{H}\mathbf{q} \quad . \quad (25)$$

For this model, the matrix \mathbf{S}_{pp} is written by

$$\mathbf{S}_{pp} = \begin{bmatrix} S_{11} & S_{12} & S_{13} \\ S_{12}^* & S_{22} & S_{23} \\ S_{13}^* & S_{23}^* & S_{33} \end{bmatrix} , \quad (26)$$

where superscript $*$ denotes complex conjugate. Since there is only one source, it is sufficient to use only one reference microphone (we will discuss in detail in section 6 how to choose the number of reference microphones when there are more sources). In such a case, \mathbf{S}_{RR} consists of (1,1) component of \mathbf{S}_{pp} , \mathbf{S}_{RM} comprises (1,2) and (1,3) components of \mathbf{S}_{pp} , and \mathbf{S}_{MM} consists of (2,2), (2,3), (3,2), and (3,3) components of \mathbf{S}_{pp} .

Now we wish to show how the submatrix \mathbf{S}_{MM} is calculated from the measured submatrices \mathbf{S}_{RR} and \mathbf{S}_{RM} . At first, we measure one auto-spectrum S_{11} at the field point 1 and two cross-spectra S_{12} and S_{13} at the field points 1, 2 and 1, 3. In this case, the matrices \mathbf{S}_1 , \mathbf{S}_2 are given by

$$\mathbf{S}_1 = \begin{bmatrix} S_{11} \\ S_{12}^* \\ S_{13}^* \end{bmatrix}, \quad \mathbf{S}_2 = \begin{bmatrix} S_{12} & S_{13} \\ S_{22} & S_{23} \\ S_{23}^* & S_{33} \end{bmatrix}. \quad (27, 28)$$

(Note that although here \mathbf{S}_1 is not a matrix but a vector, we still use uppercase representing a matrix, in order to match the notation given in section 2). For this model, the rank of \mathbf{S}_1 is unity because the dimension of \mathbf{S}_1 is 3-by-1. Also, the rank of \mathbf{S}_{pp} is determined by considering the relationship, $\mathbf{H}\mathbf{S}_{qq}\mathbf{H}^H = \mathbf{S}_{pp}$ (see equations (6) and (7)), between the cross-spectral matrix \mathbf{S}_{qq} of acoustic source spectra and the cross-spectral matrix \mathbf{S}_{pp} of acoustic pressures. In this model, the dimensions of \mathbf{H} and \mathbf{S}_{qq} are respectively 3-by-1 and 1-by-1 (i.e., scalar) and thus their ranks are one. Accordingly, the rank of \mathbf{S}_{pp} is one. Consequently, the assumption of rank equality between \mathbf{S}_1 and \mathbf{S}_{pp} is validated by using only one reference microphone. Note that in section 5 we will describe how we estimate the rank of \mathbf{S}_{pp} from $\mathbf{H}\mathbf{S}_{qq}\mathbf{H}^H = \mathbf{S}_{pp}$ for matrices of larger dimensions.

The dimension of \mathbf{S}_2 is 3-by-2 and its rank must be equal to two (i.e., full rank) or less than two (i.e., rank-deficient). However, for this model, the rank of submatrix \mathbf{S}_2 is unity, because the rank of the entire matrix \mathbf{S}_{pp} is unity. Recall that the rank a matrix is defined as the order of the largest non-singular square submatrix which can be formed by selecting rows and columns of this matrix. According to equation (20), \mathbf{S}_2 can be expressed as \mathbf{S}_1 and \mathbf{T} and thus

$$\mathbf{S}_2 = \begin{bmatrix} S_{12} & S_{13} \\ S_{22} & S_{23} \\ S_{23}^* & S_{33} \end{bmatrix} = \begin{bmatrix} S_{11} \\ S_{12}^* \\ S_{13}^* \end{bmatrix} \mathbf{T} = \mathbf{S}_1 \mathbf{T}. \quad (29)$$

The matrix \mathbf{T} is calculated by using the generalised inverse of \mathbf{S}_1 , i.e., $\mathbf{T} = \mathbf{S}_1^+ \mathbf{S}_2$.

Since $(\mathbf{S}_1^H \mathbf{S}_1)$ is not singular, $\mathbf{S}_1^+ = (\mathbf{S}_1^H \mathbf{S}_1)^{-1} \mathbf{S}_1^H$ and therefore

$$\mathbf{T} = \frac{\begin{bmatrix} S_{11}S_{12} + S_{12}S_{22} + S_{13}S_{23}^* & S_{11}S_{13} + S_{12}S_{23} + S_{13}S_{33} \end{bmatrix}}{S_{11}^2 + |S_{12}|^2 + |S_{13}|^2}. \quad (30)$$

Finally the moving position auto- and cross-spectral matrix \mathbf{S}_{MM} is calculated by using equation (23). Thus

$$\mathbf{S}_{MM} = \mathbf{S}_{RM}^H \mathbf{S}_{RR}^{-1} \mathbf{S}_{RM} = \begin{bmatrix} S_{12}^* \\ S_{13}^* \end{bmatrix} \frac{1}{S_{11}} \begin{bmatrix} S_{12} & S_{13} \end{bmatrix} = \begin{bmatrix} S_{22} & S_{23} \\ S_{23}^* & S_{33} \end{bmatrix}. \quad (31)$$

This calculated \mathbf{S}_{MM} coincides with the submatrix we wish to find consisting of (2,2), (2,3), (3,2), and (3,3) components of the matrix \mathbf{S}_{pp} . The last equality of this equation is explained in the Appendix for both cases of deterministic and stationary random pressure fluctuations.

4. ESTIMATION OF THE RANK

4.1 INTRODUCTION

As described in section 2, the prerequisite for using the technique employing reference microphones is to verify the assumption of rank equality of the two matrices \mathbf{S}_1 and \mathbf{S}_{pp} . So, in association with this, it is now worthwhile to describe methods that can be used for rank estimation. When identifying the rank of a matrix, SVD is considered as the most reliable tool regardless of whether this matrix is square or rectangular (i.e., the rank of a rectangular or square matrix is equal to the number of nonzero singular values). For a square matrix, its *eigenvalue decomposition* (EVD) can also be utilised as a rank estimator (i.e., rank of a square matrix is equal to the number of nonzero eigenvalues). Other estimators, *principal component analysis* (PCA) and *virtual coherence* (VC) can also be adopted and thus in this section the application of these concepts to the identification of the rank of \mathbf{S}_{pp} is described.

4.2 PRINCIPAL COMPONENT ANALYSIS

PCA was originated by Pearson [5] and developed by Hotelling [6] for the particular purpose of analysing correlation structures. This is a statistical technique falling under the general heading of factor analysis and consists of identifying an orthogonal (or unitary) matrix which transforms the original (or physical) signals to a

new set of uncorrelated signals which are termed the *principal components*. These uncorrelated signals are linked with the original signals via linear combinations. When applying the PCA to set of spectra it is called *principal spectral analysis* (PSA).

Now we wish to determine the rank of the acoustic pressure auto- and cross-spectral matrix \mathbf{S}_{pp} by the PSA. This is based on the EVD of \mathbf{S}_{pp} and it can be expressed as [4]

$$\mathbf{Q}^H \mathbf{S}_{pp} \mathbf{Q} = \mathbf{\Lambda} , \quad (32)$$

where \mathbf{Q} is a unitary matrix containing all eigenvectors of \mathbf{S}_{pp} and $\mathbf{\Lambda}$ is the diagonal matrix consisting of the eigenvalues of \mathbf{S}_{pp} arranged in descending order. In this expression, \mathbf{S}_{pp} is said to be unitarily similar to $\mathbf{\Lambda}$ and thus the rank of \mathbf{S}_{pp} corresponds to that of $\mathbf{\Lambda}$. Recall that two “similar” matrices have the same ranks [4]. Furthermore, because $\mathbf{\Lambda}$ is diagonal, its rank is equal to the number of nonzero diagonal elements. Thus the rank of any Hermitian matrix is the total number of its nonzero eigenvalues, including repetitions. Since in our problem \mathbf{S}_{pp} is a positive semi-definite Hermitian matrix, its eigenvalues are real and non-negative and its rank obtained by the PSA is the number of nonzero eigenvalues identified by its EVD. The matrix $\mathbf{\Lambda}$ is regarded as the matrix of the *principal auto-spectra of virtual acoustic pressures* which are mutually uncorrelated because off-diagonal terms of $\mathbf{\Lambda}$ are all zeros. Accordingly, the rank of \mathbf{S}_{pp} is equal to the number of principal auto-spectra of virtual acoustic pressures. The principal components of \mathbf{S}_{pp} , namely the principal auto-spectra of virtual acoustic pressures can also be interpreted as the components of the total energy.

4.3 VIRTUAL COHERENCE

Coherence functions such as ordinary, partial and multiple coherence are very useful tools for the problem of vibration and noise source identification [7]. In practice, however, the approaches using these functions have some limitations. For example, the ordinary coherence function cannot be used in identifying sources for systems with partially coherent sources. It is also difficult to apply the partial coherence function to attributing energy from particular sources to the output when we

have no prior knowledge of the system such as the number of sources present in the system. The multiple coherence function can be employed to attribute parts of coherent output energy to particular sources only when sources are incoherent with each other. For this reason, the VC was developed to describe a system in which all inputs may be partially or fully coherent with each other and the nature of the signals is not well known.

The ordinary coherence function is utilised in order to apportion the measured output power to the inputs that are assumed to be totally independent. Most signals, however, are not independent in practice. Accordingly, after transforming these signals into mutually uncorrelated signals (these are virtual signals) by PSA, then we can employ the concept of the ordinary coherence function. VC is defined as the ordinary coherence function between the virtual signal and original (or physical) signal as follows. Equation (32) can be rewritten as

$$\mathbf{S}_{pp} = \mathbf{Q}\mathbf{\Lambda}\mathbf{Q}^H. \quad (33)$$

Any square matrix can be expressed by the EVD and also the SVD, and since \mathbf{S}_{pp} is a square positive semi-definite Hermitian matrix, its eigenvalues are equal to its singular values. So equation (33) can also be expressed as

$$\mathbf{S}_{pp} = \mathbf{Q}\mathbf{\Sigma}\mathbf{Q}^H, \quad (34)$$

where $\mathbf{\Sigma}$ is the matrix consisting of the singular values of \mathbf{S}_{pp} on its diagonal and as stated before, these values are tantamount to the principal auto-spectra of virtual acoustic pressures. We now denote \mathbf{v} as the column vector comprising virtual acoustic pressures. Thus

$$\mathbf{v} = \begin{bmatrix} v_1(\omega) \\ v_2(\omega) \\ \vdots \\ v_v(\omega) \end{bmatrix}, \quad (35)$$

where $v_i(\omega)$ denotes the i th virtual acoustic pressure at a particular frequency ω and subscript v is the total number of virtual acoustic pressures. The virtual and physical

acoustic pressure vectors, \mathbf{v} and \mathbf{p} , can be interpreted as the input and the output respectively. In this case if we use a unitary matrix \mathbf{Q} as the transfer function relating these, it follows that

$$\mathbf{p} = \mathbf{Q}\mathbf{v} \quad , \quad (36)$$

and

$$\mathbf{S}_{pp} = \mathbf{Q}\mathbf{S}_{vv}\mathbf{Q}^H \quad , \quad (37)$$

where \mathbf{S}_{pp} is the auto- and cross-spectral matrix of the “physical” acoustic pressures and \mathbf{S}_{vv} is the auto-spectral matrix of the “virtual” acoustic pressures. Comparing equations (33), (34) and (37), it is appreciated that $\mathbf{S}_{vv} = \mathbf{\Lambda} = \mathbf{\Sigma}$. Also, the cross-spectral matrix \mathbf{S}_{vp} between the virtual and physical acoustic pressures is related to the matrix \mathbf{S}_{vv} by

$$\mathbf{S}_{vp} = \mathbf{S}_{vv} \mathbf{Q}^H \quad . \quad (38)$$

Therefore the virtual coherence, defined as $\gamma_{v_i p_j}^2(\omega)$, between the virtual acoustic pressure $v_i(\omega)$ and the physical acoustic pressure $p_j(\omega)$ can be expressed as

$$\gamma_{v_i p_j}^2(\omega) = \frac{|S_{v_i p_j}(\omega)|^2}{S_{v_i v_i}(\omega) S_{p_j p_j}(\omega)} \quad , \quad (39)$$

where $S_{v_i v_i}(\omega)$ corresponds to the i th component of the singular value matrix $\mathbf{\Sigma}$ or the eigenvalue matrix $\mathbf{\Lambda}$ of \mathbf{S}_{pp} . In other words, $\gamma_{v_i p_j}^2(\omega)$ indicates the degree to which $S_{p_j p_j}(\omega)$ results from the virtual acoustic pressure $v_i(\omega)$. Note that $\gamma_{v_i p_j}^2(\omega)$ has the value between 0 and 1, and the summation of the contributions of all virtual signals to the j th physical signal is 1, that is, $\sum_{i=1}^V \gamma_{v_i p_j}^2(\omega) = 1$. Note also that if the sum of parts (say, K) of V virtual coherences with respect to a physical signal approaches unity it indicates that there are K dominant uncorrelated signals.

5. RELATION BETWEEN THE RANK OF ACOUSTIC PRESSURE CROSS- SPECTRAL MATRIX AND THE NUMBER OF UNCORRELATED ACOUSTIC SOURCES

It has been seen from the considerations presented above that the rank of a cross-spectral matrix indicates the number of uncorrelated signals. As described before, in a system with n acoustic source strengths \mathbf{q} which may be mutually uncorrelated or correlated and m acoustic pressures \mathbf{p} , the relationship between the cross-spectral matrices of \mathbf{q} and \mathbf{p} is expressed as $\mathbf{S}_{pp} = \mathbf{H} \mathbf{S}_{qq} \mathbf{H}^H$. In this equation, the rank of \mathbf{S}_{qq} indicates the number of uncorrelated acoustic source strengths and the rank of \mathbf{S}_{pp} is determined by the nature of the matrix \mathbf{H} . In other words, if \mathbf{H} is of full rank, then the rank of \mathbf{S}_{pp} is equal to that of \mathbf{S}_{qq} . Note that premultiplication or postmultiplication of any matrix by any non-singular (i.e., full rank) matrix does not alter its rank [8]. Thus, if m microphones are geometrically arranged for \mathbf{H} to be of full rank, the rank of \mathbf{S}_{pp} will correspond to the number of uncorrelated acoustic source strengths. Meanwhile, comparing $\mathbf{S}_{pp} = \mathbf{H} \mathbf{S}_{qq} \mathbf{H}^H$ and $\mathbf{S}_{pp} = \mathbf{Q} \mathbf{\Lambda} \mathbf{Q}^H$ (equation (33)), there is an obvious similarity between these. In association with $\mathbf{S}_{pp} = \mathbf{Q} \mathbf{\Lambda} \mathbf{Q}^H$, it was stated that the rank of \mathbf{S}_{pp} was equal to the rank of $\mathbf{\Lambda}$, without any constraint, because of the fact that \mathbf{Q} is a unitary matrix and so is of full rank. In the relationship $\mathbf{S}_{pp} = \mathbf{H} \mathbf{S}_{qq} \mathbf{H}^H$, the matrix \mathbf{H} is used in a similar fashion to the matrix \mathbf{Q} used in the relationship $\mathbf{S}_{pp} = \mathbf{Q} \mathbf{\Lambda} \mathbf{Q}^H$. Therefore, based on the similar reasoning, it can be understood again that the rank of \mathbf{S}_{pp} corresponds to the rank of \mathbf{S}_{qq} if and only if \mathbf{H} is of full rank.

6. RANK EQUALITY AND THE CHOICE OF THE NUMBER OF REFERENCE MICROPHONES

This section is devoted to a discussion of which submatrix of \mathbf{S}_{RR} and \mathbf{S}_{RM}^H determines the rank of \mathbf{S}_1 . Also, a method is proposed for the selection of the optimal number of reference positions (or microphones) which ensures the rank equality

between the matrices \mathbf{S}_{pp} and \mathbf{S}_1 and thus enables the construction of the full acoustic pressure cross-spectral matrix \mathbf{S}_{pp} with minimum measurement effort.

Let us first consider the definition of \mathbf{S}_1 given by equation (16). The dimension of \mathbf{S}_1 is m -by- u with $u < m$ (recall that m and u represent the entire number of microphones and the number of reference microphones, respectively) and thus $\text{rank}(\mathbf{S}_1) \leq u$. In addition, \mathbf{S}_1 consists of two submatrices, \mathbf{S}_{RR} (u -by- u) and \mathbf{S}_{RM}^H (v -by- u) (equation (16)). Therefore when $u < v$, $\text{rank}(\mathbf{S}_{RR}) \leq u$, $\text{rank}(\mathbf{S}_{RM}^H) \leq u$, when $u > v$, $\text{rank}(\mathbf{S}_{RR}) \leq u$, $\text{rank}(\mathbf{S}_{RM}^H) \leq v$, and when $u = v$, $\text{rank}(\mathbf{S}_{RR}) \leq u$, $\text{rank}(\mathbf{S}_{RM}^H) \leq u$. (Recall that if a matrix \mathbf{A} is of m -by- n , $\text{rank}(\mathbf{A}) \leq \min(m, n)$).

Now we wish to check which of two submatrices, \mathbf{S}_{RR} and \mathbf{S}_{RM} , determines the rank of \mathbf{S}_1 . Note that the rank of \mathbf{S}_{RM}^H corresponds to that of \mathbf{S}_{RM} because an elementary operation such as conjugate transpose does not alter the rank of a matrix. Firstly, it should be pointed out that the case of $u > v$ is unusual. In such a case the number of reference microphones is larger than that of the moving microphones and is of little practical relevance, although we have considered this case here for the sake of completeness. Denoting the number of uncorrelated sources as w , we can consider five possible combinations of u , v and w : $w > u > v$, $u > v > w$, $u > w > v$, $w = u > v$, $u > v = w$. For these, ranks of the matrices of \mathbf{S}_{RR} , \mathbf{S}_{RM} , \mathbf{S}_1 , and \mathbf{S}_{pp} are given by cases 1 to 5 of Table 1. In computing these ranks, we have to recall two things. One is that rank of the cross-spectral matrix is the same as the number of the uncorrelated sources. The other is that in such a case as $u > v$, $\text{rank}(\mathbf{S}_{RR}) \leq u$ and $\text{rank}(\mathbf{S}_{RM}) \leq v$. Secondly, for the case of $u < v$ (this is the usual case), $\text{rank}(\mathbf{S}_{RR}) \leq u$ and $\text{rank}(\mathbf{S}_{RM}) \leq u$. In this case, there are also five possible combinations of u , v and w : $u < v < w$, $w < u < v$, $u < w < v$, $w = u < v$, and $u < v = w$. The ranks of the matrices of \mathbf{S}_{RR} , \mathbf{S}_{RM} , \mathbf{S}_1 , and \mathbf{S}_{pp} are given by cases 6 to 10 of Table 1. Finally, for the case of $u = v$, we can consider three possible combinations of u , v and w : $u = v = w$, $u = v < w$, and $u = v > w$. The ranks of the matrices \mathbf{S}_{RR} , \mathbf{S}_{RM} , \mathbf{S}_1 , and \mathbf{S}_{pp} are given by cases 11 to 13 of Table 1. According to Table 1, it is evident that $\text{rank}(\mathbf{S}_1)$ is always the same as $\text{rank}(\mathbf{S}_{RR})$.

Table 1. Ranks of \mathbf{S}_{RR} , \mathbf{S}_{RM} , \mathbf{S}_{pp} , and \mathbf{S}_1 , where u , v and w are the number of reference microphones, moving microphones, and uncorrelated acoustic sources, respectively.

	Case No.	No. of microphones		Ranks of matrices			
		u	v	\mathbf{S}_{RR}	\mathbf{S}_{RM}	\mathbf{S}_{pp}	\mathbf{S}_I
$u > v$	1	$w > u$	$w > v$	u	v	w	u
	2	$w < u$	$w < v$	w	w	w	w
	3	$w < u$	$w > v$	w	v	w	w
	4	$w = u$	$w > v$	w	v	w	w
	5	$w < u$	$w = v$	w	w	w	w
$u < v$	6	$w > u$	$w > v$	u	u	w	u
	7	$w < u$	$w < v$	w	w	w	w
	8	$w > u$	$w < v$	u	u	w	u
	9	$w = u$	$w < v$	w	u	w	w
	10	$w > u$	$w = v$	u	u	w	u
$u = v$	11	$w = u$	$w = u$	w	w	w	w
	12	$w > u$	$w > u$	u	u	w	u
	13	$w < u$	$w < u$	w	w	w	w

An example of the determination of the ranks of \mathbf{S}_{RR} , \mathbf{S}_{RM} , \mathbf{S}_I , and \mathbf{S}_{pp} with different number of reference and moving microphones (i.e., u and v) is shown in Table 2. These results have been obtained from numerical simulations using the model of Figure 2. In this model it is assumed that there are four mutually uncorrelated acoustic point monopoles radiating sound in a free field. For the cases 2, 3, 5, 7, 8, 9, we use this model with sixteen microphones. For the cases 1, 4, 6, 10, five microphones (numbered 1 to 5) are used. Also, we use this model with eight microphones (numbered 1 to 8), six microphones (numbered 1 to 6), and ten microphones (numbered 1 to 10) for the cases 11, 12, 13, respectively. In this model, the four sources are made “mutually uncorrelated” (i.e., $w=4$) by assigning four different normally distributed random signals having variances $\sigma_1^2=1$, $\sigma_2^2=4$, $\sigma_3^2=9$, and $\sigma_4^2=16$ as four acoustic source strengths. It also is assumed in this model that there is no output noise. As an example, consider the case of $u=5$ and $v=11$ (case 7). In this case the ranks of \mathbf{S}_{RR} and \mathbf{S}_{RM} will be less than or equal to 5. However, since the number of uncorrelated acoustic source strengths is 4, the ranks of these two matrices

can not exceed 4. Also, since the rank of the cross-spectral matrix equals the number of uncorrelated sources, the ranks of these two matrices both become 4. The other cases can be explained similarly.

Table 2. Ranks of \mathbf{S}_{RR} , \mathbf{S}_{RM} , \mathbf{S}_{pp} , and \mathbf{S}_l obtained using the models of Figure 2, where the number of uncorrelated source strengths is 4 (i.e., $w=4$).

	Case No.	No. of microphones		Ranks of matrices			
		u	v	\mathbf{S}_{RR}	\mathbf{S}_{RM}	\mathbf{S}_{pp}	\mathbf{S}_l
$u > v$	1	3	2	3	2	4	3
	2	11	5	4	4	4	4
	3	13	3	4	3	4	4
	4	4	1	4	1	4	4
	5	12	4	4	4	4	4
$u < v$	6	2	3	2	2	4	2
	7	5	11	4	4	4	4
	8	3	13	3	3	4	3
	9	4	12	4	4	4	4
	10	1	4	1	1	4	1
$u = v$	11	4	4	4	4	4	4
	12	3	3	3	3	4	3
	13	5	5	4	4	4	4

Therefore, it is clear that the rank of \mathbf{S}_l is determined by the rank of \mathbf{S}_{RR} . Thus in order to prove the rank equality of \mathbf{S}_l and \mathbf{S}_{pp} , it is necessary to choose the number of reference microphones appropriately. As a consequence, since the rank of \mathbf{S}_{pp} is equal to the number of uncorrelated sources, w , the number u of reference microphones must be equal to or more than w . This can be checked from the cases 2, 3, 4, 5, 7, 9, 11, and 13 of Tables 1 and 2. In other words, since the rank of \mathbf{S}_{pp} equals the number of significant singular values, we have to choose the number of reference microphones to be equal to or greater than the number of the significant singular values of \mathbf{S}_{pp} .

It should now be noted that the application of this conclusion regarding the number of required reference microphones is not difficult in a “forward problem” in which we have prior knowledge of the number of uncorrelated acoustic sources.

However it is in general problematic in an “inverse problem” because the number of uncorrelated sources is unknown. Accordingly, in order to properly select the number of reference microphones in an inverse problem, we propose the following approach. At first, select P reference microphones and then calculate the rank of \mathbf{S}_{RR} obtained from measurements. For convenience denote this rank as K_P . After that, decrease the number of reference microphones by 1, i.e., $P-1$ and calculate again the rank of \mathbf{S}_{RR} and denote this rank as K_{P-1} . Then check whether K_P and K_{P-1} correspond to each other or not:

- 1) If K_P and K_{P-1} are equal, repeat the further decrease of the number of reference microphones and calculation of rank of \mathbf{S}_{RR} until K_{P-i} and K_{P-i-1} become different. If this occurs, then K_{P-i} is the number of significant singular values of \mathbf{S}_{pp} and thus is the required number of reference microphones which provides the rank equality of \mathbf{S}_1 and \mathbf{S}_{pp} and at the same time the minimum number of measurements of acoustic pressure cross-spectra;
- 2) If K_P and K_{P-1} differ, increase P by 1, and calculate again the rank of \mathbf{S}_{RR} , which is denoted by K_{P+1} . Check whether K_P and K_{P+1} are the same. If so, K_P is the number of significant singular values of \mathbf{S}_{pp} and is thus equal to the required number of reference microphones. If this is not so, repeat the further increase of the number of reference microphones and calculation of rank of \mathbf{S}_{RR} until K_{P+i} and K_{P+i+1} become equal. If this happens, then K_{P+i} is the number of significant singular values of \mathbf{S}_{pp} and therefore the optimal number of reference microphones which we wish to find.

Consider a simple example using the model of Figure 2. Assume that there are four uncorrelated acoustic sources and thus four significant singular values of \mathbf{S}_{pp} . In addition, no output noise is assumed. As a first trial, we select 7 reference microphones and find the rank of \mathbf{S}_{RR} , which is denoted by K_7 . Then decrease the number of reference microphones by 1, i.e., 6, and find again the rank of \mathbf{S}_{RR} , which is denoted by K_6 . In this case, $K_7=K_6=4$. So, repeat the further decrease of the number of

reference microphones and identification of the rank of \mathbf{S}_{RR} . Finally, we can find $K_4 (=4) \neq K_3 (=3)$ and therefore we can realise that the required number of reference microphones is 4. Now let us consider the case in which we use 2 reference microphones, instead of 7 reference microphones, as a first trial. Calculate the rank of \mathbf{S}_{RR} , which is denoted by K_2 . Then reduce the number of reference microphones by 1, i.e., to 1, and calculate the rank of \mathbf{S}_{RR} , which is denoted by K_1 . Comparing K_2 and K_1 reveals $K_2 (=2) \neq K_1 (=1)$. Accordingly, increase the initial number of reference microphones by 1, i.e., to 3, and calculate the rank of \mathbf{S}_{RR} , which is denoted by K_3 . Check whether K_2 and K_3 are the same. In this case, $K_2=2$ and $K_3=3$ and so they are different. Repeat the further increase of the number of reference microphones and calculation of rank of \mathbf{S}_{RR} . In the final analysis, we can identify $K_4=K_5=4$ and therefore we can recognise that the required number of reference microphones is 4.

7. SIMULATION RESULTS I : NO MEASUREMENT NOISE

7.1 UNCORRELATED ACOUSTIC SOURCE STRENGTHS

To clarify some features of the theory developed above, we conduct a set of computer simulations. The first simulation is carried out using the model illustrated in Figure 2. Recall that in this model four acoustic sources are made “mutually uncorrelated” by assigning four different normally distributed random signals having variances, $\sigma_1^2=1$, $\sigma_2^2=4$, $\sigma_3^2=9$ and $\sigma_4^2=16$ as the four acoustic source strengths. It is also assumed in this model that there is no measurement noise. Before we calculate the matrix \mathbf{S}_{MM} from the measured matrices \mathbf{S}_{RR} and \mathbf{S}_{RM} , we first have to check the rank equality of \mathbf{S}_1 and \mathbf{S}_{pp} given by equation (19). As already mentioned, the rank of \mathbf{S}_1 is determined by the rank of \mathbf{S}_{RR} and the number of necessary reference microphones has to be at least equal to the number of uncorrelated acoustic sources or the number of significant singular values of \mathbf{S}_{pp} (here it is 4). Comparison of the ranks of \mathbf{S}_{pp} and \mathbf{S}_1 plotted in the left hand part of Figure 3 supports this statement.

The effect of the number of reference microphones on the accuracy of the calculation of \mathbf{S}_{MM} is now investigated. As a measure of accuracy of calculation, we

use the normalised difference R_1 between the directly measured and calculated \mathbf{S}_{MM} defined as

$$R_1 = \frac{\|\mathbf{S}_{MM}^{\text{mea}} - \mathbf{S}_{MM}^{\text{cal}}\|_e}{\|\mathbf{S}_{MM}^{\text{mea}}\|_e}, \quad (40)$$

where subscripts $_{\text{mea}}$ and $_{\text{cal}}$ denote “measured” and “calculated” and $\|\cdot\|_e$ denotes the Euclidean norm of the matrix. Note that, strictly speaking, in the simulation results the terms “measured” and “calculated” mean “directly calculated” and “estimated”, respectively. The results of the right hand part of Figure 3 reveal that the accurate calculation of \mathbf{S}_{MM} can be achieved only when the rank equality between \mathbf{S}_{pp} and \mathbf{S}_1 is satisfied. That is, when using 3 reference microphones, the normalised difference R_1 is over 10^{-3} , whilst for the cases of using 4 or 5 reference microphones it is below 10^{-11} . On the other hand, the fact that the rank of \mathbf{S}_{pp} is 4 also indicates that there exist 4 principal auto-spectra of virtual acoustic pressures. The result of Figure 4 emphasises this point. The rank of \mathbf{S}_{pp} can also be identified from the VC. The results of Figure 5 illustrate the VC for the 1st, 2nd, 3rd and 4th virtual acoustic pressure with respect to the 1st physical acoustic pressure. Their sum is unity and this signifies that there are no other virtual acoustic pressures. It is therefore concluded that the rank of this model is 4.

From the results of Figure 3, we select four microphones as reference microphones (or reference positions) for the model of Figure 2. In this case, the dimensions of the matrices \mathbf{S}_{RR} , \mathbf{S}_{MM} and \mathbf{S}_{pp} are 4-by-4, 12-by-12 and 16-by-16, respectively. Based on the rank equality of \mathbf{S}_{pp} and \mathbf{S}_1 , we can now estimate \mathbf{S}_{MM} using equation (23). The results of Figure 6 illustrate that acoustic pressure auto- and cross-spectra estimated at the 5th and 8th positions which correspond respectively the 1st and 4th moving positions are in good agreement with those calculated directly. The normalised difference R_1 reveals that there is a successful prediction for all moving positions. Also, Figure 6 shows the normalised difference matrix \mathbf{R}_2 defined by

$$\mathbf{R}_2 = \frac{|\mathbf{S}_{MM}^{\text{mea}} - \mathbf{S}_{MM}^{\text{cal}}|}{|\mathbf{S}_{MM}^{\text{mea}}|}, \quad (41)$$

where $||$ denotes the absolute value. The values presented in Figure 6 are for $kr_{ss}=1.65$ ($=600\text{Hz}$, $r_{ss}=0.15\text{m}$). According to the above results, it is obvious that the technique using reference microphones to construct the full auto- and cross-spectral matrix of \mathbf{S}_{pp} is reliable in accuracy. For the simulation model of Figure 2, while direct measurements of acoustic pressure auto- and cross-spectra are required 136 ($=16 \times 17/2$) times, when we use this technique the number of required measurements is only 58 ($=4 \times 5/4 + 4 \times 12$). So this technique is seen to be a fast and economic tool for obtaining the full auto- and cross-spectral matrix \mathbf{S}_{pp} of acoustic pressures.

7.2 CORRELATED ACOUSTIC SOURCE STRENGTHS

Now consider the case of a model having correlated sources. As an example, we use a simply supported plate mounted in an infinite baffle as shown in Figure 7. The plate is excited at a point by a normally distributed random force. As a result, the surface velocities of the plate generate the acoustic field. The plate is discretised into 16 contiguous small rectangular elements each of which is regarded as a point monopole source. It is also assumed that there is no output noise.

Since a single force excites this plate, it is anticipated that there may exist only one uncorrelated acoustic source among 16 discretised acoustic sources. So we use only one microphone numbered by 1 in Figure 7 as the reference microphone. Thus, the rank of \mathbf{S}_1 is equal to that of \mathbf{S}_{pp} and they are of rank 1. It means that there will be one principal auto-spectra of \mathbf{S}_{pp} and this is ensured from Figure 8. Thus, there exists only 1 virtual acoustic pressure. Figure 9 illustrates the virtual coherence of the virtual acoustic pressure with respect to the physical acoustic pressure sensed at the microphone numbered by 1 in Figure 7. Only 1 virtual acoustic pressure has unity as the value of virtual coherence. Note that the virtual coherence with respect to the physical acoustic pressures sensed at the other microphones showed the same results, although they are not presented here. With the achievement of rank equality, the estimated magnitudes and phases of the components of \mathbf{S}_{MM} exhibit an excellent agreement with the directly calculated values, as plotted in Figure 10. Note also that auto- and cross-spectra of Figure 10 were obtained from the acoustic pressures

normalised by unit force and so the shape is smooth despite the excitation by a normally distributed random force.

From the results presented up to now, it is clear that the technique using reference microphones is applicable regardless of the nature of sources (i.e., uncorrelated or correlated). In addition, this technique will be more advantageous for models having highly correlated sources rather than that having fully uncorrelated sources, because the former requires fewer reference microphones, compared with the latter.

8. SIMULATION RESULTS II: WITH OUTPUT NOISE

We now investigate the performance of the technique using reference microphones for a more realistic model where output noise contaminates the acoustic pressures. In measuring the cross-spectral matrices, we make an assumption that the output noise is independent, identically distributed for all sensors, and additive. This implies that the noise will be equally distributed over all the components of \mathbf{S}_{pp} . Accordingly, the matrix \mathbf{S}_{pp} and its submatrices \mathbf{S}_{RR} , \mathbf{S}_{RM} , \mathbf{S}_{MM} , \mathbf{S}_1 , and \mathbf{S}_2 are transformed into $\mathbf{S}_{\hat{p}\hat{p}}$, $\mathbf{S}_{\hat{R}\hat{R}}$, $\mathbf{S}_{\hat{R}\hat{M}}$, $\mathbf{S}_{\hat{M}\hat{M}}$, \mathbf{S}_1^{\wedge} , and \mathbf{S}_2^{\wedge} , respectively (where \wedge signifies data contaminated by the output noise). From these measured matrices $\mathbf{S}_{\hat{R}\hat{R}}$ and $\mathbf{S}_{\hat{R}\hat{M}}$, the moving position auto- and cross-spectral matrix $\mathbf{S}_{\hat{M}\hat{M}}$ is obtained by following the procedure used in reaching equation (23) or (24). Thus when the matrix $\mathbf{S}_{\hat{R}\hat{R}}$ is of full rank

$$\mathbf{S}_{\hat{M}\hat{M}} = \mathbf{S}_{\hat{R}\hat{M}}^H \mathbf{S}_{\hat{R}\hat{R}}^{-1} \mathbf{S}_{\hat{R}\hat{M}} \quad , \quad (42)$$

or when the matrix $\mathbf{S}_{\hat{R}\hat{R}}$ is rank-deficient

$$\mathbf{S}_{\hat{M}\hat{M}} = \mathbf{S}_{\hat{R}\hat{M}}^H \mathbf{S}_{\hat{R}\hat{R}}^{+} \mathbf{S}_{\hat{R}\hat{M}} \quad . \quad (43)$$

8.1 UNCORRELATED ACOUSTIC SOURCE STRENGTHS

In order to observe the effect of output noise corrupting the acoustic pressures on the accuracy of calculation of the moving position auto- and cross-spectral matrix, the model shown in Figure 2 is again used. Output noise is added into all components of acoustic pressure auto- and cross-spectra \mathbf{S}_{pp} . Like the previous case which was not concerned with the effect of noise, we select 4 reference microphones as a first trial. (Recall that in the absence of output noise, the use of 4 reference microphones provided a good estimation of \mathbf{S}_{MM} , as illustrated in Figure 6). In this case, the rank of $\mathbf{S}_{\hat{p}\hat{p}}$ is 5 (note that the rank of \mathbf{S}_{pp} was 4) whilst the rank of $\mathbf{S}_{\hat{1}}$ still is kept unchanged 4 because 4 reference microphones are used. The change of rank of the matrix $\mathbf{S}_{\hat{p}\hat{p}}$ is of course the consequence of the addition of output noise auto-spectra. In other words, the number of significant singular values (Figure 11) of the matrix $\mathbf{S}_{\hat{p}\hat{p}}$ increases to 5 from the value of 4 associated with the matrix \mathbf{S}_{pp} (Figure 4) because of the addition of output noise. The failure to verify the assumption of rank equality between $\mathbf{S}_{\hat{1}}$ and $\mathbf{S}_{\hat{p}\hat{p}}$ by using only 4 reference microphones makes the estimated magnitudes and phases of the components of $\mathbf{S}_{\hat{M}\hat{M}}$ deviate from the directly calculated values, as illustrated in Figure 12. Also, the measure of deviation of all components of $\mathbf{S}_{\hat{M}\hat{M}}$ with frequency can be observed from the normalised difference R_1 . The quantity of R_1 (i.e., $10^{-2} \sim 1$) plotted in Figure 12 is much larger than that of R_1 (i.e., $10^{-14} \sim 10^{-11}$) shown in Figure 6 in which the rank equality between $\mathbf{S}_{\hat{1}}$ and $\mathbf{S}_{\hat{p}\hat{p}}$ was verified. Figure 12 also shows the normalised difference R_2 ($\sim 10^{-1}$) is much larger than that ($\sim 10^{-12}$) of Figure 6.

Since these unsatisfactory results come from the discrepancy of two ranks of $\mathbf{S}_{\hat{1}}$ and $\mathbf{S}_{\hat{p}\hat{p}}$, we have to alter the number of reference microphones and now 5 reference microphones are selected instead of 4. As pointed out earlier, since rank of $\mathbf{S}_{\hat{1}}$ is the same as that of $\mathbf{S}_{\hat{R}\hat{R}}$, the use of 5 reference microphones yields a submatrix $\mathbf{S}_{\hat{1}}$ of rank 5. Therefore ranks of $\mathbf{S}_{\hat{1}}$ and $\mathbf{S}_{\hat{p}\hat{p}}$ become equal. Subsequently, the estimated

magnitudes and phases of components of $\mathbf{S}_{\hat{M}\hat{M}}$ are now in very good agreement with those directly calculated values (Figure 13).

8.2 CORRELATED ACOUSTIC SOURCE STRENGTHS

Finally, we consider the simply supported plate model depicted in Figure 7 which has correlated sources. For this model, measurement noise is also added. When the number of reference microphones is chosen to be 1 as before, a discrepancy appears in the ranks of $\mathbf{S}_{\hat{1}}$ and $\mathbf{S}_{\hat{p}\hat{p}}$. That is, the addition of output noise forces the rank of $\mathbf{S}_{\hat{p}\hat{p}}$ to increase to 2. The reason for this can easily be understood from viewing the singular values of $\mathbf{S}_{\hat{p}\hat{p}}$ shown in Figure 14. Hence, the estimation of the magnitudes and phases are inaccurate, as illustrated in Figure 15. Accordingly, in order to make two ranks of $\mathbf{S}_{\hat{1}}$ and $\mathbf{S}_{\hat{p}\hat{p}}$ equal, 2 reference microphones are used. As a result, the rank equality is achieved and a satisfactory estimation of $\mathbf{S}_{\hat{M}\hat{M}}$ is made as illustrated in Figure 16.

Consequently, it is apparent from the above results that the proper choice of the number of reference microphones is at the heart of this technique. If this is achieved, the construction of full auto- and cross-spectral matrix of acoustic pressures can be made faster whilst maintaining accuracy.

9. EXPERIMENTAL VERIFICATION

We now wish to verify the technique using reference microphones through the experiments, describing some practical considerations. We will use two experimental systems which were explained in details in references [9, 10]. One is the system used for the reconstruction of the strengths of two volume velocity sources (Figure 17) and the other for the reconstruction of the volume velocities of the randomly vibrating simply supported plate mounted in a finite baffle (Figure 18).

Before conducting the experimental verification, we here consider carefully the estimate of the rank of matrix $\mathbf{S}_{\hat{p}\hat{p}}$ which consists of experimental data. As pointed

out earlier, the reliable rank estimator of a matrix is the SVD. That is, the rank of a matrix is the number of singular values larger than a threshold level. Accordingly, since this threshold level plays a role of distinguishing the significant singular values from the negligible singular values, the determination of this level is important in rank estimation. In general, in the rank calculation using the data in connection with the numerical simulations, the threshold level is chosen based on the machine epsilon of the computer used (refer to [11]).

However, as far as measured data are concerned, such a threshold level is not suitable, because, for example, the quantisation error related to the analogue-to-digital converter used in the data acquisition process is, in general, larger than this machine epsilon (see reference [12], for example). Accordingly, it is reasonable to choose the threshold level, considering this kind of uncontrollable error from the practical point of view. Otherwise, we may make a mistake in determining the rank of $\mathbf{S}_{\hat{\mathbf{r}}\hat{\mathbf{r}}}$ from examining its singular value distribution. Another parameter that makes difficult the determination of the rank of matrix $\mathbf{S}_{\hat{\mathbf{r}}\hat{\mathbf{r}}}$ by viewing its singular values is the signal processing technique usually used to obtain the acoustic pressure auto- and cross-spectra. As is well known, when auto- and cross-spectra are estimated by the segment averaging method, a large number of data segments are necessary to reduce the random error. Also a long data segment is required to reduce the bias error. Thus, we cannot help but identify incorrectly the significant singular values from the cross-spectral matrix $\mathbf{S}_{\hat{\mathbf{r}}\hat{\mathbf{r}}}$ having random error and bias error. Kompella *et al* [12] studied the effect of the number of data segments and segment length on the singular values, in connection with the determination of the number of incoherent sources contributing to the response of a system. They reached similar conclusions regarding the number of data segments and the segment length. In addition, attention has to be paid to acquiring acoustic pressures with good signal-to-noise ratio. Otherwise, as described earlier, it becomes problematic to identify correctly the number of significant singular values due purely to the uncorrelated acoustic sources since background noise also modifies the magnitudes of the singular values of $\mathbf{S}_{\hat{\mathbf{r}}\hat{\mathbf{r}}}$.

However, our purpose is the identification of the required number of reference microphones necessary to secure the rank equality between the matrices $\mathbf{S}_{\hat{\mathbf{i}}}$ and $\mathbf{S}_{\hat{\mathbf{p}}\hat{\mathbf{p}}}$

by inspecting the significant singular values of the matrix $\mathbf{S}_{\hat{\mathbf{R}}\hat{\mathbf{R}}}$. Accordingly, even if there exist spurious significant singular values which result from imperfect measurement, we have to choose the reference microphones to be equal to or greater than the number of (true and spurious) significant singular values. This is borne out by the computer simulations presented previously.

With these considerations in mind, let us consider the first experimental system shown in Figure 17. Six microphones are placed to sense the acoustic pressures radiated by two volume velocity sources which are driven by one random noise generator. Since we use only one random noise generator, it is expected that this model has one significant singular value (or one significant principal auto-spectrum of virtual acoustic pressure). This is ensured from the singular value distributions of $\mathbf{S}_{\hat{\mathbf{p}}\hat{\mathbf{p}}}$ shown in Figure 19. Also observing the virtual coherence (Figure 20) of the virtual acoustic pressure with respect to the physical pressure measured at a microphone (Figure 17) reveals that there exists only one uncorrelated acoustic source. That is the 1st of six virtual coherences is very close to unity. Accordingly, we use one reference microphone (so the ranks of $\mathbf{S}_{\hat{\mathbf{R}}\hat{\mathbf{R}}}$ and $\mathbf{S}_{\hat{\mathbf{I}}}$ are one) and estimate the moving microphone auto- and cross-spectra $\mathbf{S}_{\hat{\mathbf{M}}\hat{\mathbf{M}}}$. As can be seen from Figure 21, the estimated magnitudes and phases of some components of $\mathbf{S}_{\hat{\mathbf{M}}\hat{\mathbf{M}}}$ shows good agreement with the directly measured values.

Now consider the experimental model of the randomly vibrating simply supported plate mounted in a finite baffle shown in Figure 18. (see reference [9] for details). We use four microphones to measure the acoustic pressures radiated by the plate excited by one electromagnetic driver. Thus we can think that this system has one uncorrelated acoustic source and thus the rank of matrix $\mathbf{S}_{\hat{\mathbf{p}}\hat{\mathbf{p}}}$ will be one. However, whereas the number of uncorrelated acoustic sources is obviously one, judging the rank of this matrix from its singular value distributions (Figure 22) is not straightforward. Among four singular values of $\mathbf{S}_{\hat{\mathbf{p}}\hat{\mathbf{p}}}$, whilst the 3rd and 4th singular values are relatively small, the 2nd singular value seems to be significant at some frequencies, for example, at about 310-350Hz and 420-480Hz. Although the 1st singular value is associated with one uncorrelated acoustic source, the 2nd singular

value is not. The latter is possibly due to “measurement noise” caused by acoustic reflections. This can be readily understood by viewing the geometrical placement of the microphones shown in Figure 18 which are 0.166m away from the plate. Accordingly, a spurious significant singular value is produced. The fact that there are two significant singular values (true and spurious) at those frequencies is also observed from the virtual coherences shown in Figure 23. The sum of the 1st and 2nd virtual coherences with respect to the acoustic pressure sensed at microphone 1 (Figure 18) results in nearly unity at those frequencies (the virtual coherences with respect to other acoustic pressure showed the similar results). This indicates that the rank of $\mathbf{S}_{\hat{p}\hat{p}}$ is two at those frequencies. At the other frequencies, the value of the 1st virtual coherence approaches unity, suggesting that the rank of $\mathbf{S}_{\hat{p}\hat{p}}$ is unity.

The effect of the use of one reference microphone on the estimation of $\mathbf{S}_{\hat{m}\hat{m}}$ is now investigated. The results of Figure 24 reveal that the estimated values of acoustic pressure auto-spectra at the 1st and 2nd moving microphones (corresponding to the microphone 2 and 3 in Figure 18) and magnitudes and phases of acoustic pressure cross-spectra between the 1st and 2nd moving microphones follow well the directly measured values at most frequencies. However, a discrepancy is observed at frequencies about 310-350Hz and 420-480Hz, because at those frequencies we cannot meet the requirement of the rank equality between two matrices $\mathbf{S}_{\hat{p}\hat{p}}$ and $\mathbf{S}_{\hat{1}}$ by only one reference microphone. That is to say, as could be seen from the singular value distributions (Figure 22) and the virtual coherences (Figure 23), the rank of $\mathbf{S}_{\hat{p}\hat{p}}$ is two at those frequencies. When the number of reference microphones is increased to two, the estimated auto- and cross-spectra become closer to the directly measured values at those frequencies by the virtue of the rank equality. This point can also be observed clearly by comparing the normalised differences R_1 and R_2 of Figure 25 with those of Figure 24.

10. CONCLUSIONS

For a rapid construction of the full matrix of acoustic pressure cross-spectra, we have suggested a technique using the concept of reference microphones (or positions). This has been seen as a useful tool, because this technique enables the construction of this matrix with good precision, saving measurement effort. The use of u reference microphones and v moving microphones reduces the total number of measurements to $(u(u+1)/2)+uv$ from $(u+v)(u+v+1)/2$ (which is the number required for direct measurement, when dual channel experimental equipment is employed). This method has constructed satisfactorily the full matrix regardless of the nature of acoustic sources (correlated or uncorrelated) and also when acoustic pressure data are corrupted by noise. The prerequisite of using this technique is to validate the assumption of the rank equality between the full matrix \mathbf{S}_{pp} (or $\mathbf{S}_{\hat{p}\hat{p}}$) and its submatrix \mathbf{S}_1 (or \mathbf{S}_1). To do this, it is necessary to select properly the number of reference microphones. This is determined by knowing how many significant singular values of the matrix \mathbf{S}_{pp} (or $\mathbf{S}_{\hat{p}\hat{p}}$) are present. That is to say, the number of reference microphones should be at least equal to the number of significant singular values of the matrix \mathbf{S}_{pp} (or $\mathbf{S}_{\hat{p}\hat{p}}$). However, since we do not have information regarding the acoustic sources in the inverse problem, we have proposed a method of choosing the number of reference microphones. Regarding the choice of reference microphones, attention should be drawn to the case in which the output noise corrupts acoustic pressures. Since the output noise increases the number of significant singular values of the matrix $\mathbf{S}_{\hat{p}\hat{p}}$, compared with that of \mathbf{S}_{pp} , in this case the number of reference microphones has to be chosen by examining carefully the singular value distribution of the matrix $\mathbf{S}_{\hat{R}\hat{R}}$ of reference position auto- and cross-spectra.

ACKNOWLEDGEMENT

This research was financially supported by the Daewoo Motor Company, Korea.

REFERENCES

1. P. A. NELSON and S. H. YOON 1998 *ISVR Technical Report No. 278, University of Southampton*. Estimation of acoustic source strength by inverse methods: Part I, Conditioning of the inverse problem.
2. S. H. YOON and P. A. NELSON 1998 *Journal of Sound and Vibration*. Estimation of acoustic source strength by inverse methods: Part II, Methods for choosing regularisation parameters (submitted).
3. J. HALD 1989 *B&K Technical Review No.1* STSF-a unique technique for scan-based Near-field Acoustic Holography without restrictions on coherence.
4. S. BARNETT 1990 *Matrices: methods and applications*. Oxford University Press.
5. K. PEARSON 1901 *Philosophical Magazine* 559-572. On lines and planes of closest fit to points in space.
6. H. HOTELLING 1933 *Journal of Education Psychology*, **24**, 417-441, 498-520. Analysis of a complex of statistical variables into principal components.
7. J. S. BENDAT and A. G. PIERSON 1980 *Engineering applications of correlation and spectral analysis*. John Wiley & Sons.
8. D. F. MORRISON 1976 *Multivariate statistical methods*. McGraw-Hill, New York.
9. S. H. YOON and P. A. NELSON 1998 *ISVR Technical Report No. 280, University of Southampton*. Estimation of acoustic source strength by inverse methods: Part III, experiment.
10. S. H. YOON 1998 *PhD Thesis, University of Southampton*. Reconstruction of acoustic source strength distributions and their interactions by inverse techniques.
11. THE MATHWORKS INC. 1992 *MATLAB Reference Guide*.
12. M. S. KOMPPELLA, P. DAVIES, R. J. BERNHARD and D. A. UFFORD 1994 *Mechanical Systems and Signal Processing* **8** 363-380. A technique to determine the number of incoherent sources contributing to the response of a system.

APPENDIX: Proof of equation (31)

The last equality of equation (31) is proved. For the acoustic pressures that have a deterministic time history, we can use

$$S_{ij} = p_i p_j^* . \quad (\text{A1})$$

Note that cross-spectra S_{ij} are very often defined as $p_i^* p_j$ instead of $p_i p_j^*$. However, we have used $p_i p_j^*$ up to now (see equation (7), for example) and to keep the consistency of notation, we also use this here. As an example, the (1,1) component of \mathbf{S}_{MM} of equation (31) can be developed by using equation (A1)

$$\frac{S_{12}^* S_{12}}{S_{11}} = \frac{p_1^* p_2 p_1 p_2^*}{p_1 p_1^*} = p_2 p_2^* = S_{22} . \quad (\text{A2})$$

Other components of \mathbf{S}_{MM} can be found by the same manner.

For the acoustic pressures that have a time dependence which can be regarded as stationary random, the above method is not applicable because

$$\frac{S_{12}^* S_{12}}{S_{11}} = \frac{E[p_1^* p_2] E[p_1 p_2^*]}{E[p_1 p_1^*]} \neq \frac{E[p_1^*] E[p_2] E[p_1] E[p_2^*]}{E[p_1] E[p_1^*]} . \quad (\text{A3})$$

Note that $E[p_1^* p_2]$ and $E[p_1 p_2^*]$ cannot be expressed as $E[p_1^*] E[p_2]$ and $E[p_1] E[p_2^*]$ because p_1 and p_2 result from the same source and thus they are not independent. This separation can be allowed only if two random signals are independent [13]. Accordingly, we adopt an alternative method as follows. Using equation (25), the (1,1) component of \mathbf{S}_{MM} can be developed as

$$\frac{S_{12}^* S_{12}}{S_{11}} = \frac{E[p_1^* p_2] E[p_1 p_2^*]}{E[p_1 p_1^*]} = \frac{E[H_1^* q^* H_2 q] E[H_1 q H_2^* q^*]}{E[H_1 q] E[H_1^* q^*]} . \quad (\text{A4})$$

This equation can be arranged by

$$\frac{E[H_1^* q^* H_2 q] E[H_1 q H_2^* q^*]}{E[H_1 q] E[H_1^* q^*]} = \frac{H_1^* H_2 S_{qq} H_1 H_2^* S_{qq}}{H_1 H_1^* S_{qq}} = H_2 H_2^* S_{qq}, \quad (\text{A5})$$

where $S_{qq}=E[qq^*]$. The last equation is manipulated as

$$H_2 H_2^* S_{qq} = E[H_2 q H_2^* q^*] = E[p_2 p_2^*] = S_{22}. \quad (\text{A6})$$

Therefore it is proved that

$$\frac{S_{12}^* S_{12}}{S_{11}} = S_{22}. \quad (\text{A7})$$

The same manner can be used to obtain the other components of \mathbf{S}_{MM} .

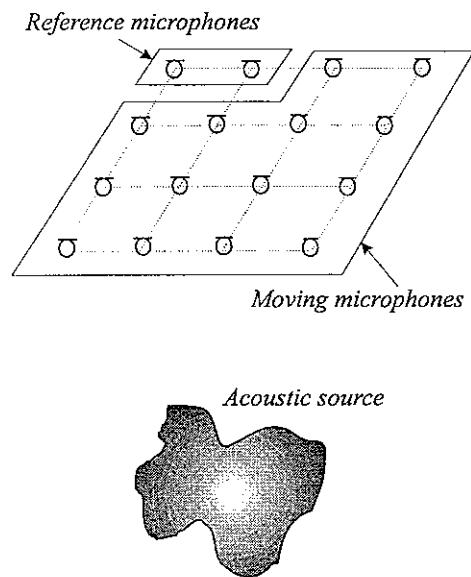


Figure 1. The partition of the entire number of measurement positions (or microphones) into the reference and moving positions (or microphones).

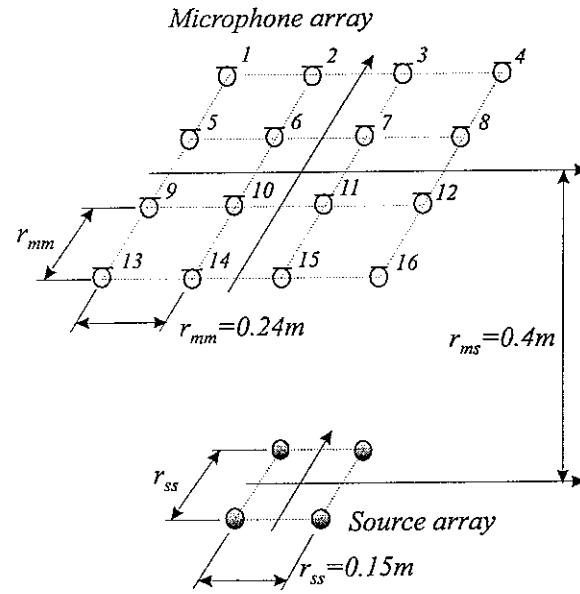


Figure 2. A simulation model for computing the ranks of \mathbf{S}_{RR} , \mathbf{S}_{RM} , \mathbf{S}_I , and \mathbf{S}_{pp} .

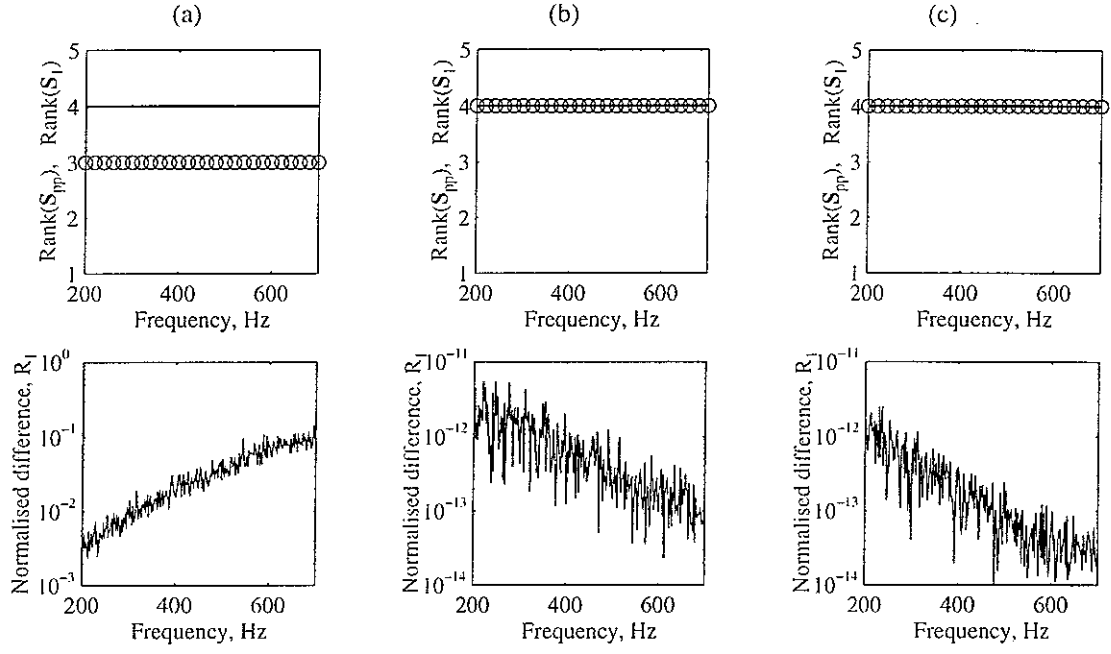


Figure 3. Effect of the number of reference microphones ((a) 3, (b) 4, (c) 5) on variations of rank of S_{pp} (solid), rank of S_l (circle) and the normalised difference R_l . There are 4 uncorrelated acoustic sources.

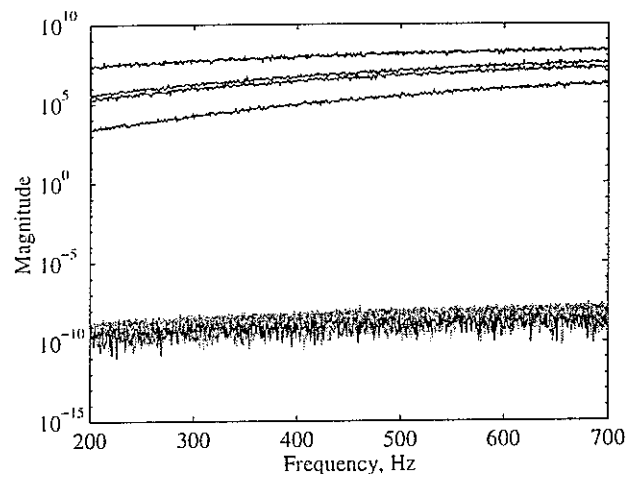


Figure 4. Principal auto-spectra (or singular values) of \mathbf{S}_{pp} for the model (Figure 2) comprising 4 uncorrelated sources under the assumption of no output noise.

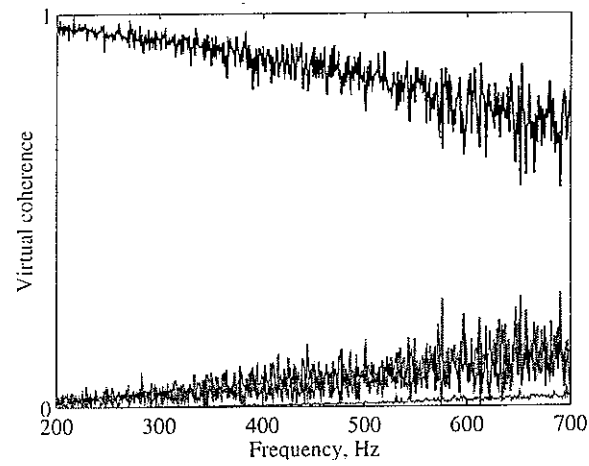


Figure 5. Virtual coherences of the 1st (black thick), the 2nd (grey thick), the 3rd (black thin), and the 4th (grey thin) virtual acoustic pressure with respect to the physical acoustic pressure sensed at the microphone 1 for the model in Figure 2 comprising 4 uncorrelated sources and the assumption of no output noise.

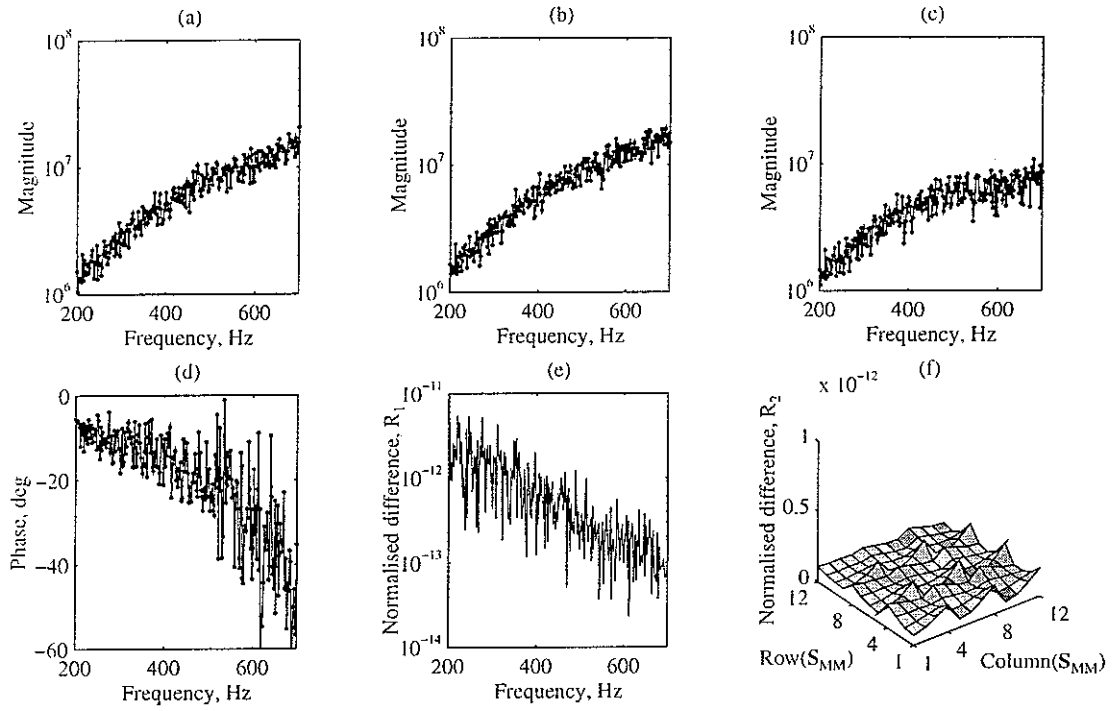


Figure 6. A comparison of the directly calculated (solid) and estimated (dotted) S_{MM} : (a) auto-spectra at the 1st moving position, (b) auto-spectra at the 4th moving position, (c) (d) magnitude and phase of cross-spectra between the 1st and 4th moving positions, (e) normalised difference R_1 , (f) normalised difference matrix R_2 at $kr_{ss}=1.65$ ($=600\text{Hz}$, $r_{ss}=0.15\text{m}$). These results are for the model of Figure 2 comprising 4 uncorrelated sources and the assumption of no output noise.

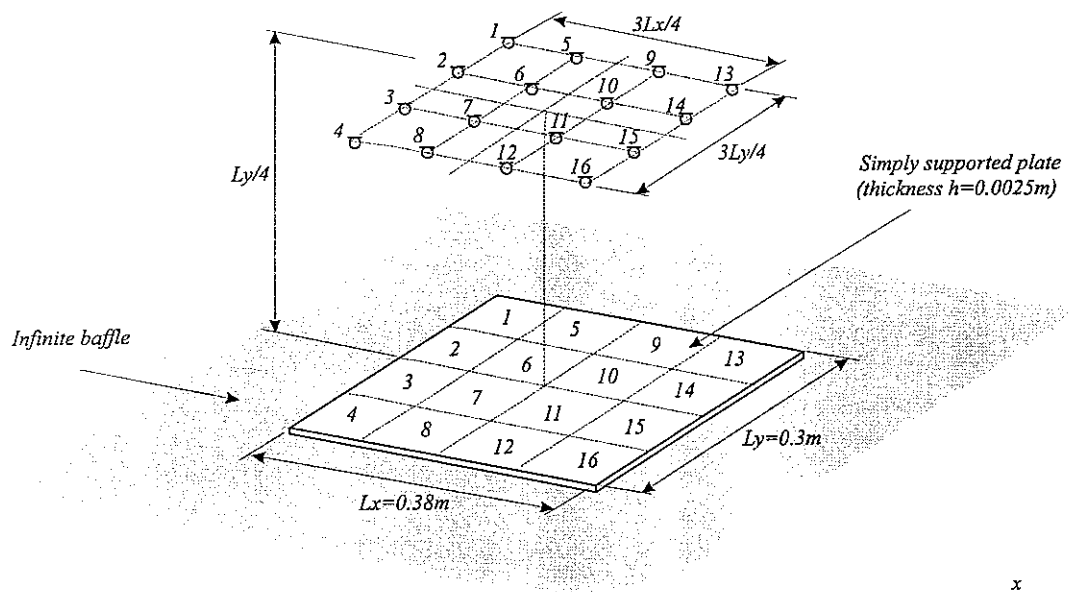


Figure 7. Geometry of a simply supported plate mounted in an infinite baffle used for the computer simulation.

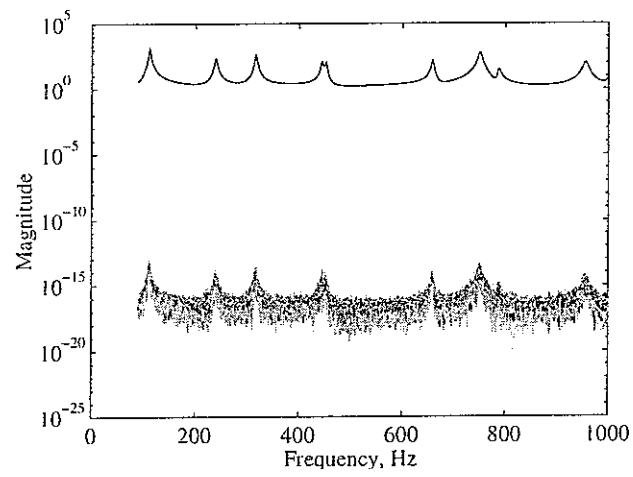


Figure 8. Principal auto-spectra (or singular values) of S_{pp} for the simply supported plate model (Figure 7) under the assumption of no output noise.

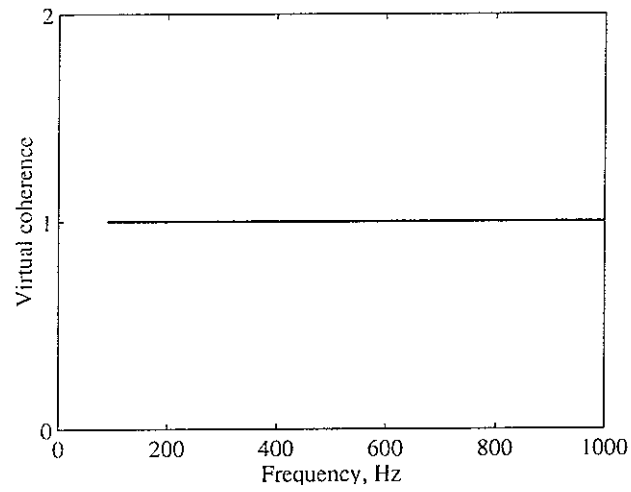


Figure 9. Virtual coherence of the virtual acoustic pressure with respect to the physical acoustic pressure sensed at the microphone 1 for the simply supported plate model (Figure 7) under the assumption of no output noise.

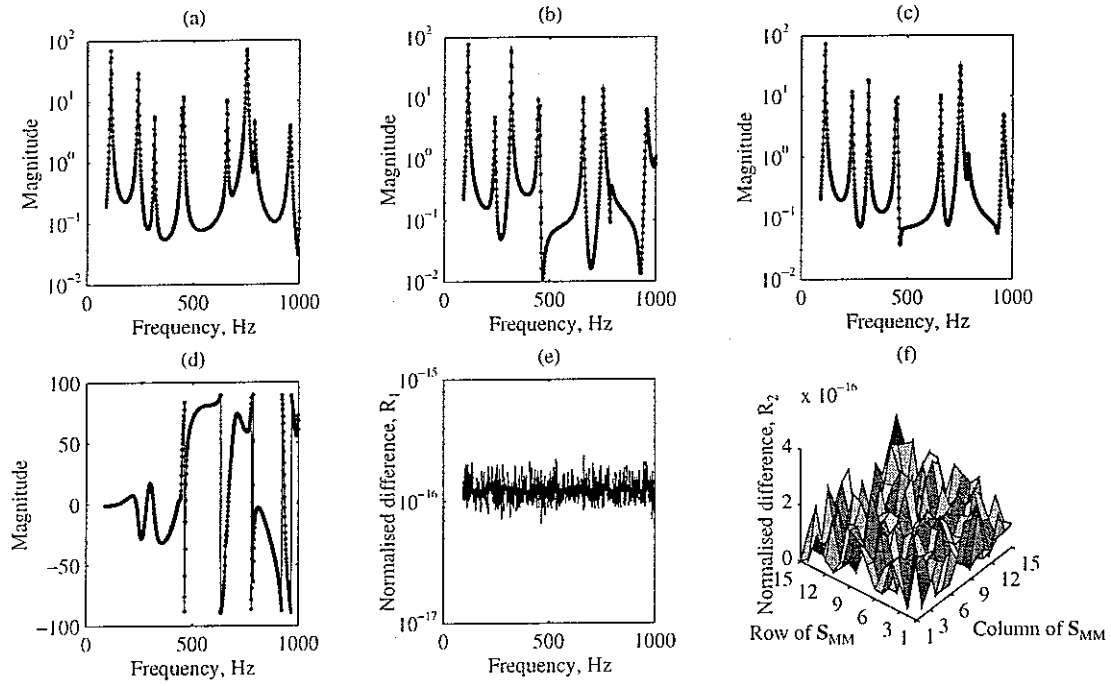


Figure 10. A comparison of the directly calculated (solid) and estimated (dotted) S_{MM} : (a) auto-spectra at the 1st moving position, (b) auto-spectra at the 4th moving position, (c) (d) magnitude and phase of cross-spectra between the 1st and 4th moving positions, (e) normalised difference R_1 , (f) normalised difference matrix R_2 at $kr_{ss}=1.37$ ($=786\text{Hz}$, $r_{ss}=0.095\text{m}$) which is the (2,3) resonant frequency. These results are for the simply supported plate model of Figure 7 under the assumption of no output noise.

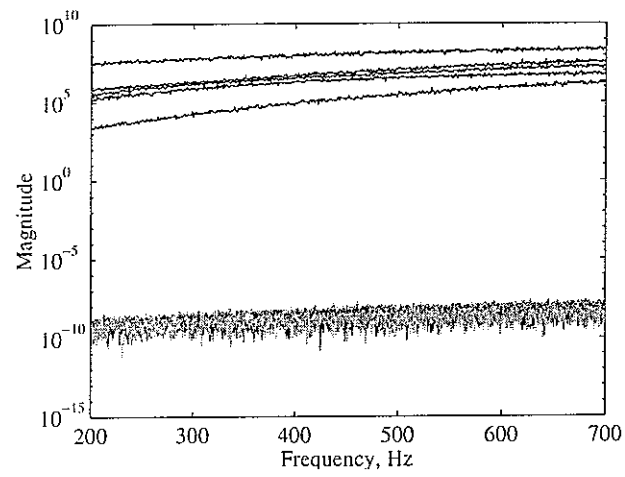


Figure 11. Principal auto-spectra (or singular values) of $\mathbf{S}_{\hat{p}\hat{p}}$ for the model of Figure 2.

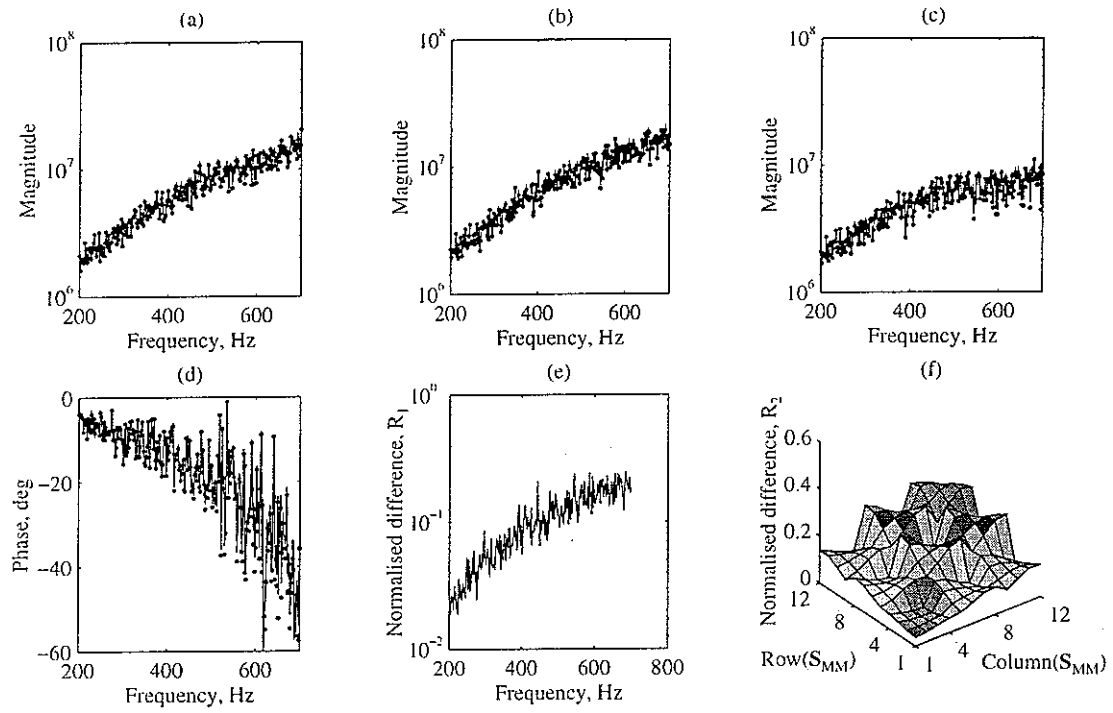


Figure 12. A comparison of the directly calculated (solid) and estimated (dotted) $S_{\hat{M}\hat{M}}$: (a) auto-spectra at the 1st moving position, (b) auto-spectra at the 4th moving position, (c) (d) magnitude and phase of cross-spectra between the 1st and 4th moving positions, (e) normalised difference R_1 , (f) normalised difference matrix \mathbf{R}_2 at $kr_{ss}=1.65$ ($=600\text{Hz}$, $r_{ss}=0.15\text{m}$) for the model of Figure 2 with output noise. Four reference microphones are used.

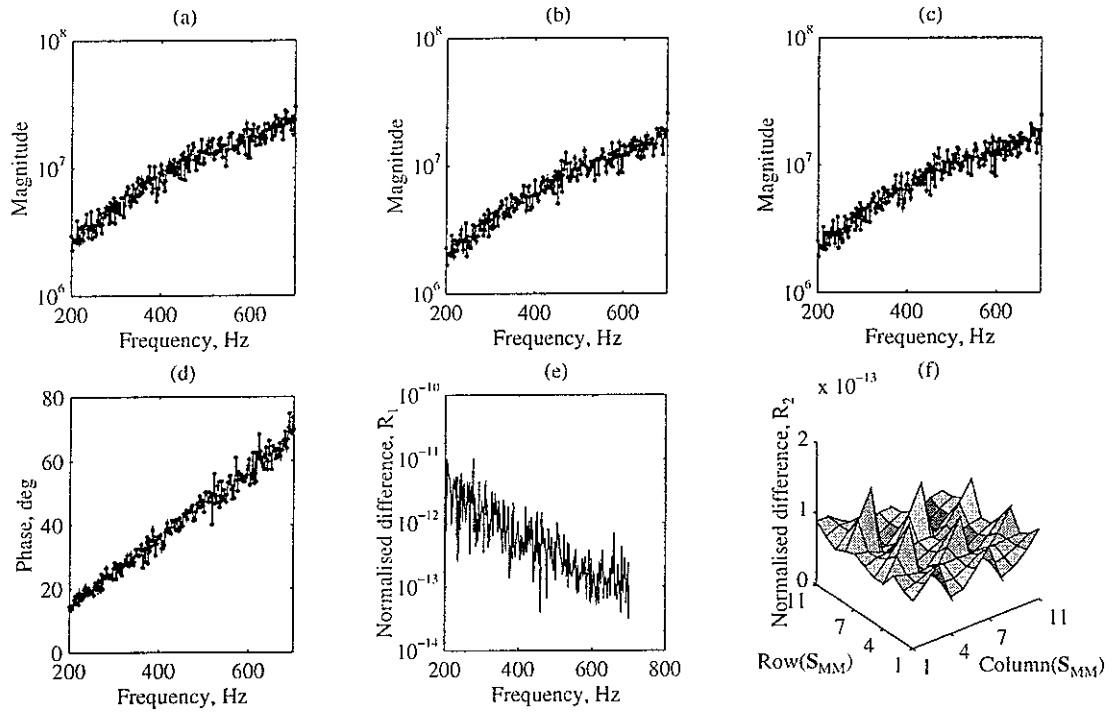


Figure 13. A comparison of the directly calculated (solid) and estimated (dotted) S_{MM} : (a) auto-spectra at the 1st moving position, (b) auto-spectra at the 4th moving position, (c) (d) magnitude and phase of cross-spectra between the 1st and 4th moving positions, (e) normalised difference R_1 , (f) normalised difference matrix \mathbf{R}_2 at $kr_{ss}=1.65$ ($=600\text{Hz}$, $r_{ss}=0.15\text{m}$). These results are for the model of Figure 2 with output noise when 5 reference microphones are used.

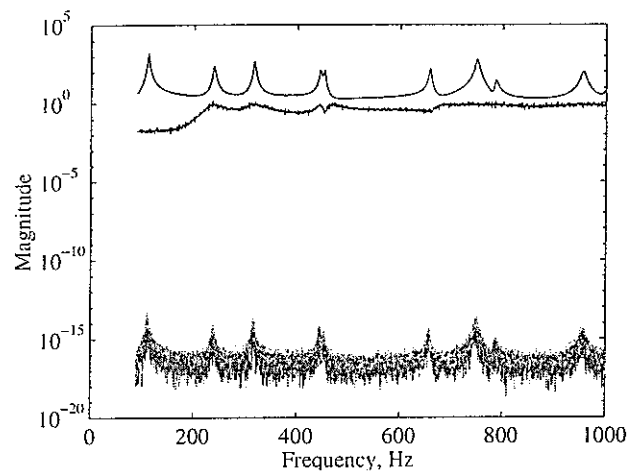


Figure 14. Principal auto-spectra (or singular values) of $\mathbf{S}_{\hat{p}\hat{p}}$ for the model of Figure 7.

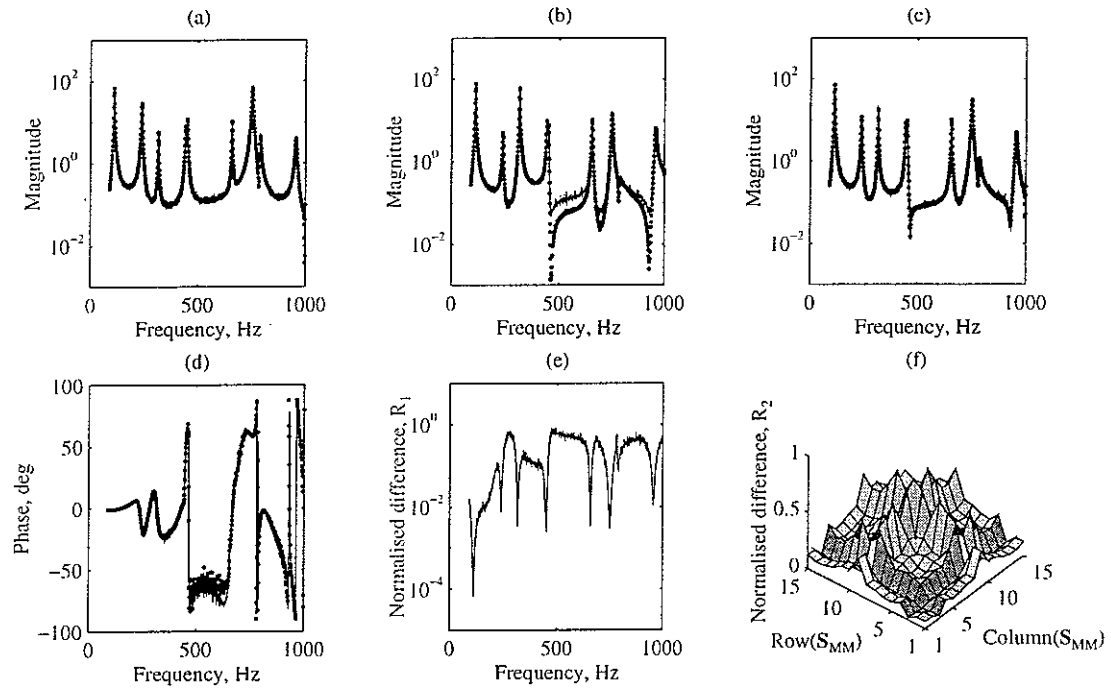


Figure 15. A comparison of the directly calculated (solid) and estimated (dotted) S_{MM} : (a) auto-spectra at the 1st moving position, (b) auto-spectra at the 4th moving position, (c) (d) magnitude and phase of cross-spectra between the 1st and 4th moving positions, (e) normalised difference R_1 , (f) normalised difference matrix \mathbf{R}_2 at $kr_{ss}=1.37$ ($=786\text{Hz}$, $r_{ss}=0.095\text{m}$) which is the (2,3) resonant frequency for the simply supported plate model of Figure 7 with output noise. One reference microphone is used.

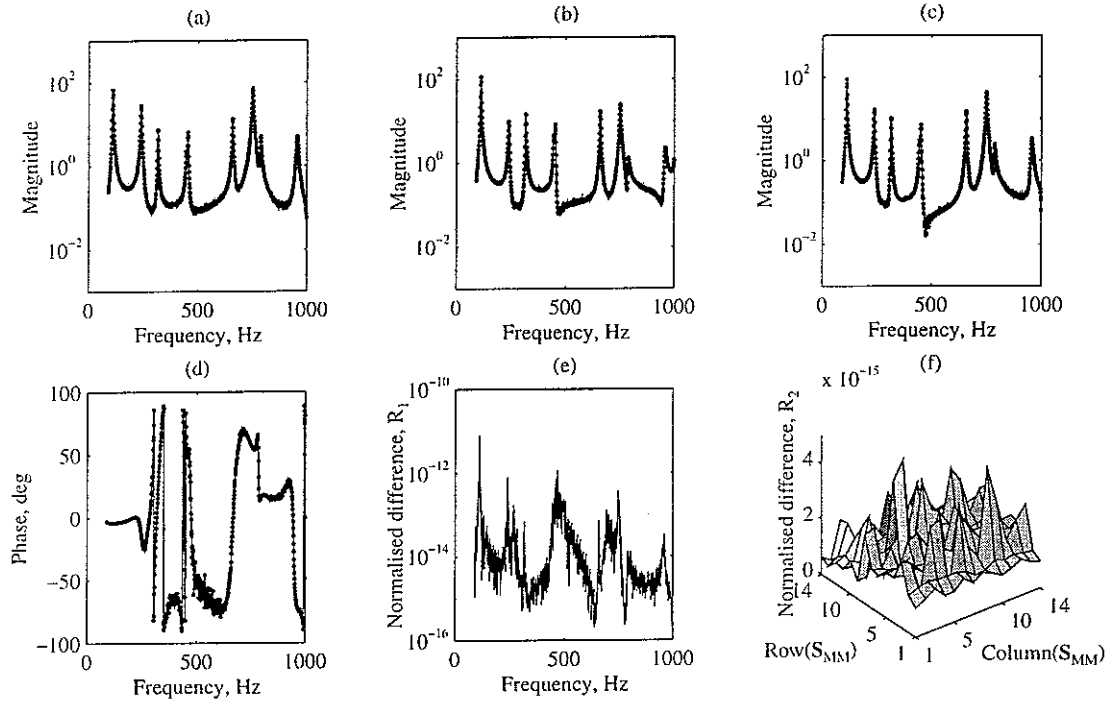


Figure 16. A comparison of the directly calculated (solid) and estimated (dotted) S_{MM} : (a) auto-spectra at the 1st moving position, (b) auto-spectra at the 4th moving position, (c) (d) magnitude and phase of cross-spectra between the 1st and 4th moving positions, (e) normalised difference R_1 , (f) normalised difference matrix R_2 at $kr_{ss}=1.37$ ($=786\text{Hz}$, $r_{ss}=0.095\text{m}$) which is the (2,3) resonant frequency. These results are for the simply supported plate model of Figure 7 with output noise. Two reference microphones are used.

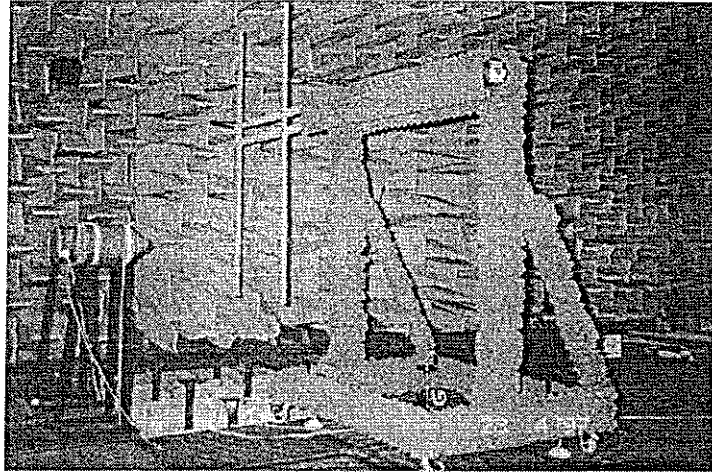


Figure 17. Experimental arrangement for the reconstruction of strengths of two volume velocity sources.

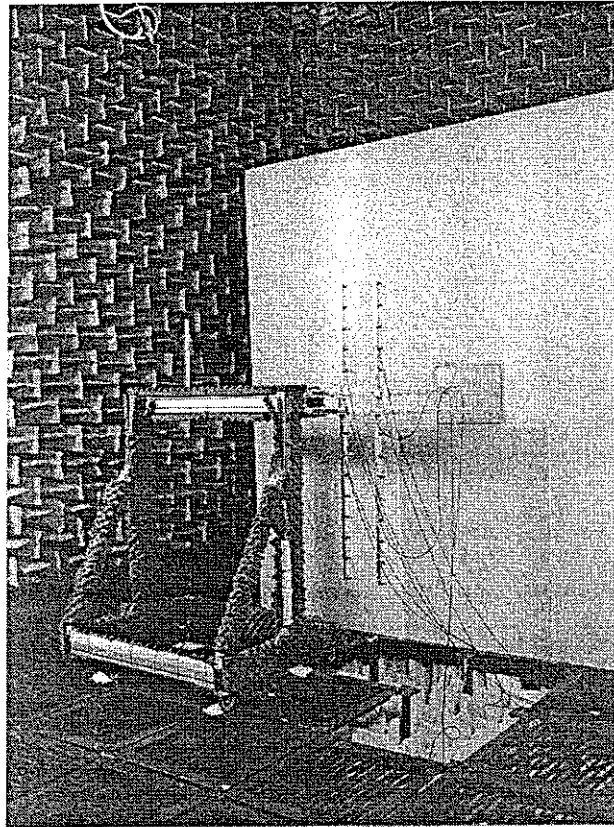


Figure 18. Experimental arrangement for the reconstruction of volume velocities of a randomly vibrating plate mounted in a finite baffle.

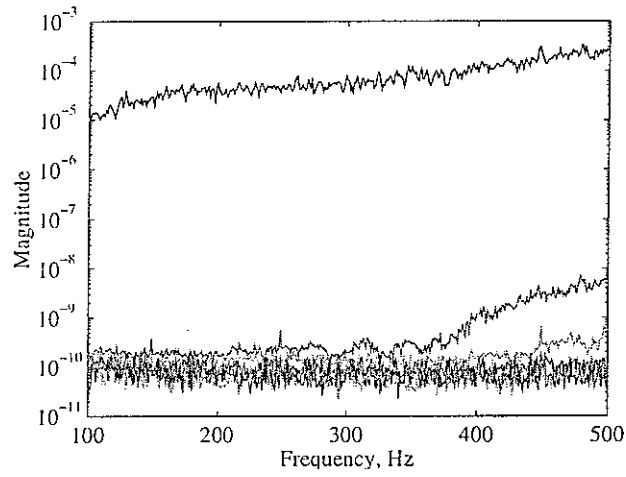


Figure 19. Six principal auto-spectra (or singular values) of $S_{\hat{p}\hat{p}}$ for the model (Figure 17) consisting of the two volume velocity sources driven by one random noise generator and six microphones.

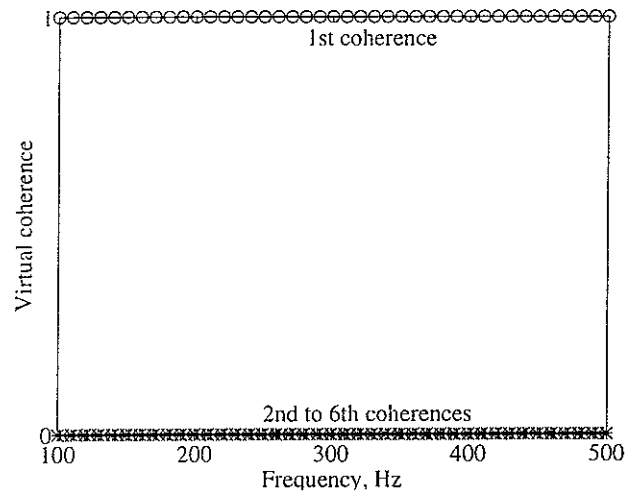


Figure 20. Virtual coherences of the 1st to 6th virtual acoustic pressure with respect to the physical acoustic pressure sensed at the microphone 1 in Figure 20(b) consisting of the two volume velocity sources driven by one random noise generator and six microphones.

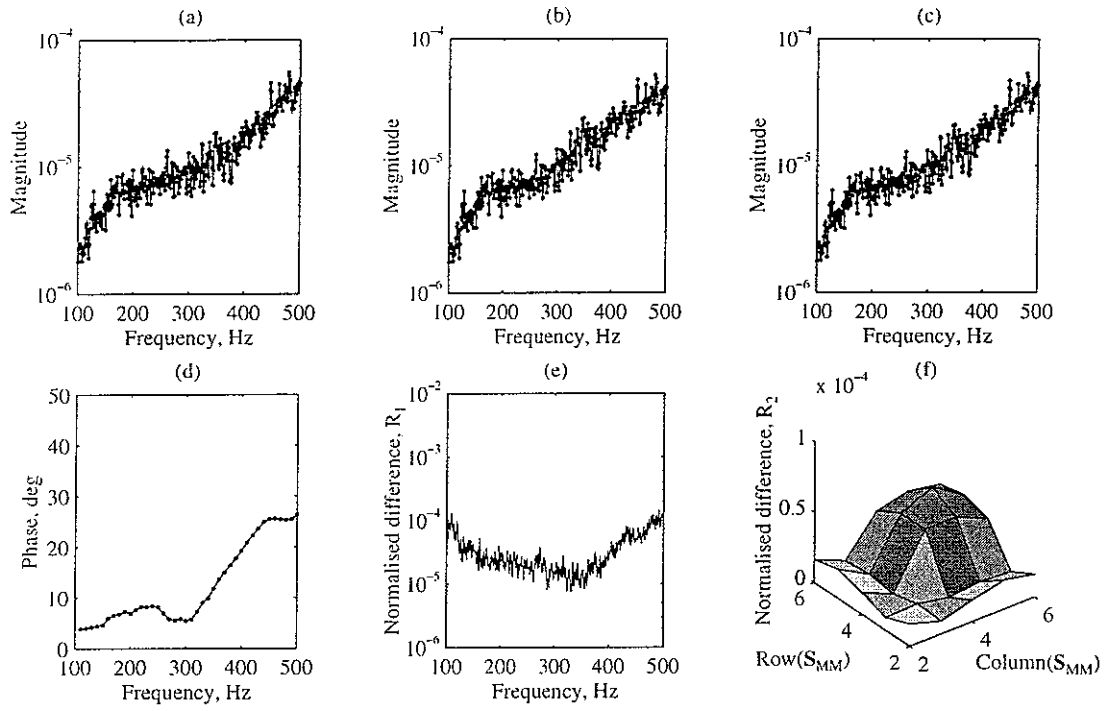


Figure 21. A comparison of the directly measured (solid) and estimated (dotted) $S_{\hat{M}\hat{M}}$: (a) auto-spectra at the 1st moving position, (b) auto-spectra at the 2nd moving position, (c) (d) magnitude and phase of cross-spectra between the 1st and 2nd moving positions, (e) normalised difference R_1 , (f) normalised difference matrix \mathbf{R}_2 at $ka=0.1$ ($=400\text{Hz}$, $a=0.014\text{m}$) for the model of Figure 17 consisting of the two volume velocity sources driven by one random noise generator and six microphones. One reference microphone is used.

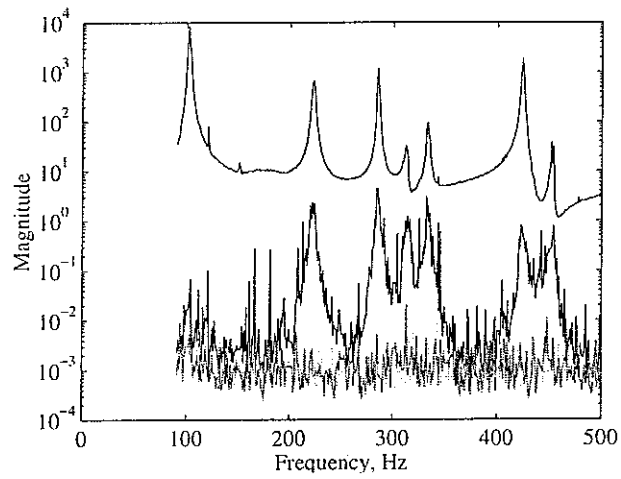


Figure 22. Principal auto-spectra (or singular values) of $S_{\hat{p}\hat{p}}$ for the model (Fig. 9.13) consisting of the simply supported plate excited by one electromagnetic driver and four microphones.

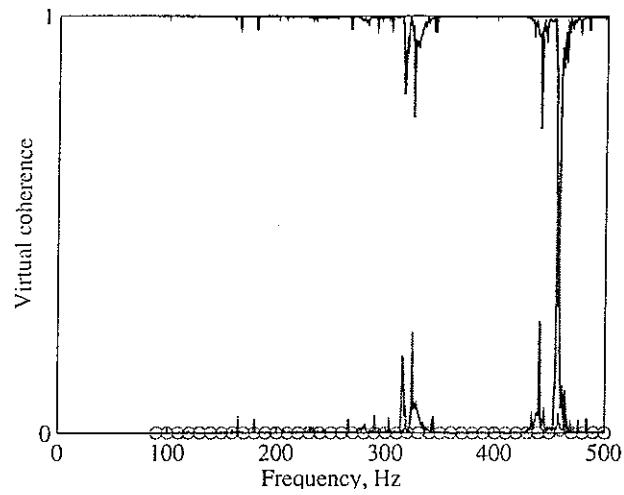


Figure 23. Virtual coherences of the 1st (black thick), the 2nd (grey thick), the 3rd (black thin), and the 4th virtual acoustic pressure (grey thin circle) with respect to the physical acoustic pressure sensed at the microphone 1 in Figure 18 consisting of the simply supported plate excited by one electromagnetic driver and four microphones.

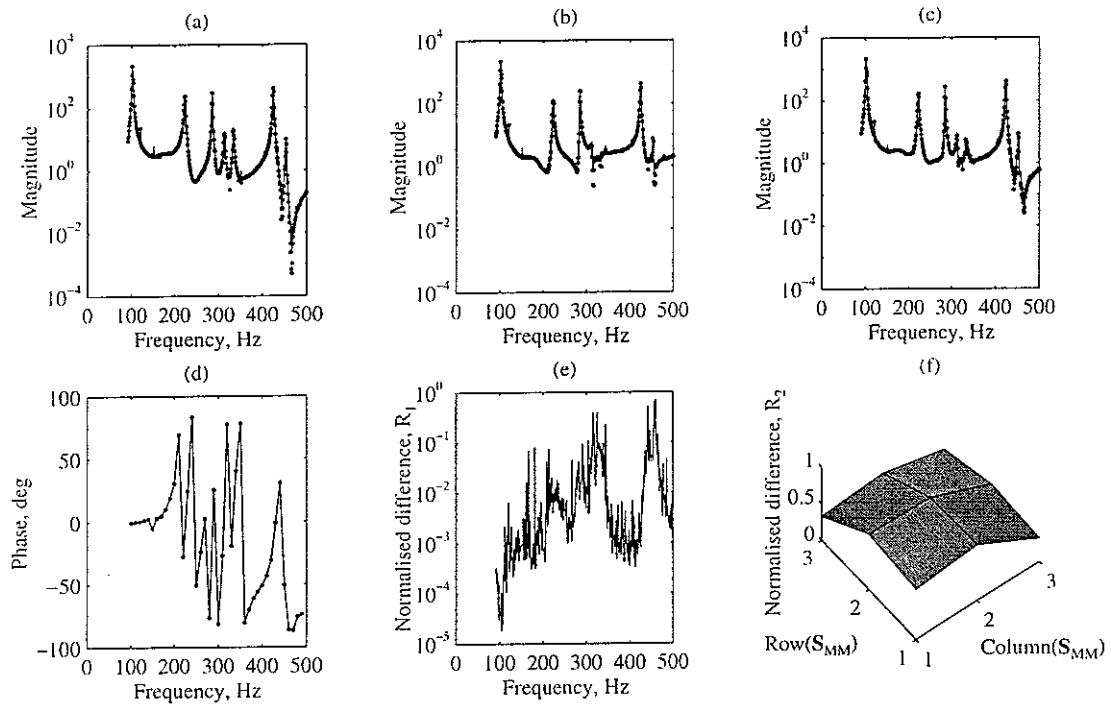


Figure 24. A comparison of the directly measured (solid) and estimated (dotted) S_{MM} : (a) auto-spectra at the 1st moving position, (b) auto-spectra at the 2nd moving position, (c) (d) magnitude and phase of cross-spectra between the 1st and 2nd moving positions, (e) normalised difference R_1 , (f) normalised difference matrix \mathbf{R}_2 at $ka=0.1$ ($=458\text{Hz}$, $a=0.014\text{m}$) for the model of Figure 18 consisting of the simply supported plate excited by one electromagnetic driver. One reference microphone is used.

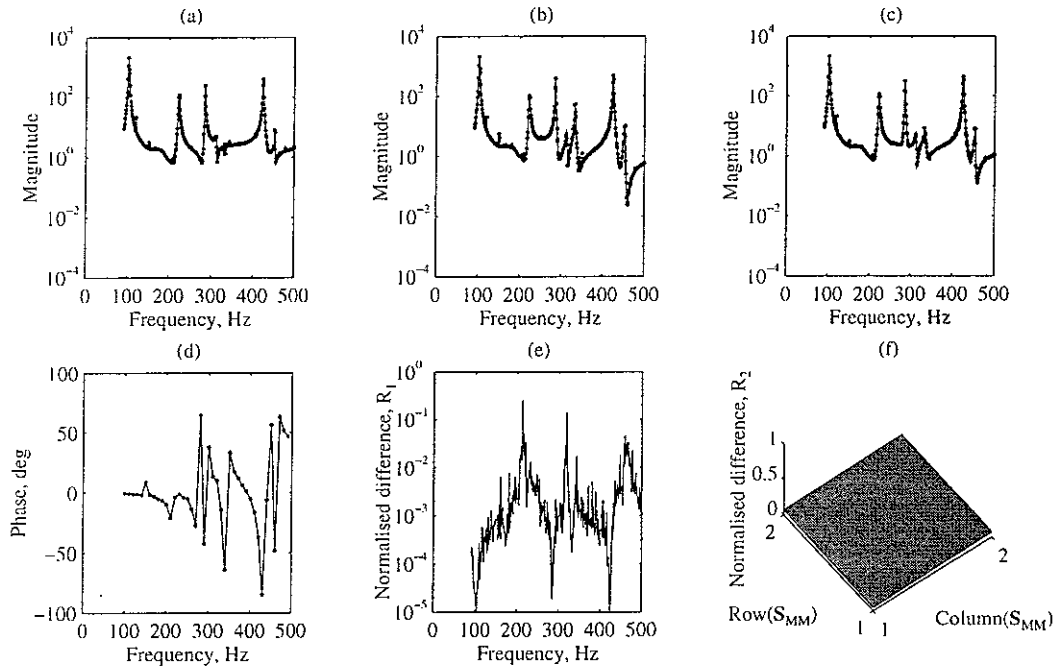


Figure 25. A comparison of the directly measured (solid) and estimated (dotted) S_{MM} : (a) auto-spectra at the 1st moving position, (b) auto-spectra at the 2nd moving position, (c) (d) magnitude and phase of cross-spectra between the 1st and 2nd moving positions, (e) normalised difference R_1 , (f) normalised difference matrix R_2 at $ka=0.1$ ($=458\text{Hz}$, $a=0.014\text{m}$) for the model of Figure 18 consisting of the simply supported plate excited by one electromagnetic driver. Two reference microphones are used.